OXFORD GENETICS

GENETICS, 2023, 224(3), iyad071
https://doi.org/10.1093/genetics/iyad071
Advance Access Publication Date: 19 April 2023
Investigation

A novel ubiquitin–proteasome system regulation of Sgf73/ataxin-7 that maintains the integrity of the coactivator SAGA in orchestrating transcription

Priyanka Barman,[1] Amala Kaja,[1,2] Pritam Chakraborty,[1] Shalini Guha,[1,‡] Arpan Roy,[1,‡] Jannatul Ferdoush,[1,3] Sukesh R. Bhaumik[1,*]

[1]Department of Biochemistry and Molecular Biology, Southern Illinois University School of Medicine, Carbondale, IL 62901, USA
[2]Department of Medicine, Baylor College of Medicine, Houston, TX-77030, USA
[3]Present address: Department of Biology, Geology, and Environmental Science, University of Tennessee at Chattanooga, 615 McCallie Ave, Chattanooga, TN 37403, USA

*Corresponding author: Tel: 618-453-6479, Email: sbhaumik@siumed.edu
‡These authors contributed equally to this work.

Abstract

Ataxin-7 maintains the integrity of *S*pt-*A*da-*G*cn5-*A*cetyltransferase (SAGA), an evolutionarily conserved coactivator in stimulating preinitiation complex (PIC) formation for transcription initiation, and thus, its upregulation or downregulation is associated with various diseases. However, it remains unknown how ataxin-7 is regulated that could provide new insights into disease pathogenesis and therapeutic interventions. Here, we show that ataxin-7's yeast homologue, Sgf73, undergoes ubiquitylation and proteasomal degradation. Impairment of such regulation increases Sgf73's abundance, which enhances recruitment of *T*ATA box-*b*inding *p*rotein (TBP) (that nucleates PIC formation) to the promoter but impairs transcription elongation. Further, decreased Sgf73 level reduces PIC formation and transcription. Thus, Sgf73 is fine-tuned by ubiquitin–proteasome system (UPS) in orchestrating transcription. Likewise, ataxin-7 undergoes ubiquitylation and proteasomal degradation, alteration of which changes ataxin-7's abundance that is associated with altered transcription and cellular pathologies/diseases. Collectively, our results unveil a novel UPS regulation of Sgf73/ataxin-7 for normal cellular health and implicate alteration of such regulation in diseases.

Keywords: ubiquitylation, proteasomal degradation, Sgf73, ataxin-7, TBP, RNA polymerase II, transcription

Introduction

Transcription is initiated via the facilitated assembly of the general transcription factors (GTFs) at the core promoter by activator proteins (Bhaumik and Malik 2008; Bhaumik 2011; Durairaj *et al.* 2017; Karmakar *et al.* 2018). Activator binds to the specific DNA sequence upstream of the core promoter to recruit coactivator that enhances the assembly of GTFs to form the preinitiation complex (PIC) for transcription initiation. A multiprotein complex, Spt-Ada-Gcn5-Acetyltransferase (SAGA), is a well-characterized and evolutionarily conserved coactivator involved in gene activation (Baker and Grant 2007; Rodriguez-Navarro 2009; Bhaumik 2011; Lee *et al.* 2011; Spedale *et al.* 2012; Soffers and Workman 2020; Chen and Dent 2021; Espinola-Lopez and Tan 2021; Grant *et al.* 2021). In yeast, SAGA contains 20 proteins that are organized into multiple modules such as *de**ub*iquitinase (DUB), *h*istone *a*cetyl*t*ransferase (HAT), *T*ATA box-*b*inding *p*rotein (*T*BP)-*a*ssociated *f*actor (TAF), and *s*uppressor of *T*y (SPT) (Baker and Grant 2007; Rodriguez-Navarro 2009; Köhler *et al.* 2010; Samara *et al.* 2010; Bhaumik 2011; Lee *et al.* 2011; Samara *et al.* 2012; Spedale *et al.* 2012; Cheon *et al.* 2020). The DUB and HAT modules have 2 distinct enzymatic activities for histone H2B deubiquitylation and histone H3 acetylation, respectively, and thus, SAGA plays important roles in regulating histone covalent modifications in addition to its well-established function in stimulation of the PIC formation via its interaction with the activator and the TBP component of the PIC (Dudley *et al.* 1999; Sterner *et al.* 1999; Brown *et al.* 2001; Bhaumik and Green 2001, 2002; Larschan and Winston 2001; Bhaumik *et al.* 2004; Sermwittayawong and Tan 2006; Shukla, Bajwa, and Bhaumik 2006; Bhaumik 2011; Shukla *et al.* 2012; Durairaj, Sen, *et al.* 2014).

The DUB module has 4 proteins, namely, Ubp8, Sgf11, Sgf73, and Sus1 (Köhler *et al.* 2010; Samara *et al.* 2010; Bhaumik 2011; Samara *et al.* 2012; Cheon *et al.* 2020). Sgf73 connects the DUB module with the rest of SAGA (Köhler *et al.* 2006, 2008; Lee *et al.* 2009; Köhler *et al.* 2010; Durand *et al.* 2014; Morgan *et al.* 2016; Wang *et al.* 2020) and, hence, maintains SAGA's overall structural integrity and DUB activity (Lee, Florens, *et al.* 2005; Shukla, Bajwa, and Bhaumik 2006; Köhler *et al.* 2010). Consistently, the loss of Sgf73 impairs SAGA's overall structural integrity (Shukla, Bajwa, and Bhaumik 2006; Köhler *et al.* 2008; Lee *et al.* 2009; Wang *et al.* 2020), PIC formation (Shukla, Bajwa, and Bhaumik 2006), and transcription (Shukla, Bajwa, and Bhaumik 2006). Thus, functional alteration/misregulation of Sgf73 is likely to develop cellular pathologies. Indeed, deletion of Sgf73 homologue in humans (known as ataxin-7/ATXN7 that maintains SAGA's integrity) is found to impair retinal development, leading to early childhood blindness (Yanicostas *et al.* 2012; Mohan, Abmayr, and Workman 2014; Mohan, Dialynas, et al. 2014; Karam and

Received: January 31, 2023. **Accepted:** March 15, 2023

Trottier 2018). Ataxin-7 is also involved in neurodegenerative diseases through the modulation of chromatin structure and gene activation (Palhan *et al.* 2005; Helmlinger, Hardy, *et al.* 2006; Garden and La Spada 2008; McCullough *et al.* 2012; Yanicostas *et al.* 2012; Mohan, Abmayr, and Workman 2014; Mohan, Dialynas, et al. 2014; Karam and Trottier 2018). Further, impairment of SAGA's DUB activity causes the defect in neuronal tube development and promotes oncogenesis (Weake *et al.* 2008; Zhang *et al.* 2008; Kapoor 2013; Schrecengost *et al.* 2014; Melo-Cardenas *et al.* 2018). Moreover, accumulation of polyglutamine-expanded ataxin-7 leads to the dysfunction and death of neurons in the retina, cerebellum, and brainstem, which cause blindness, progressive loss of coordination, and premature death (Holmberg *et al.* 1998; Lindenberg *et al.* 2000; Yvert *et al.* 2001; Yoo *et al.* 2003; Michalik *et al.* 2004; Helmlinger, Hardy, *et al.* 2006; Rüb *et al.* 2008; Karam and Trottier 2018). Furthermore, increased expression of ataxin-7 is associated with attention-deficit/hyperactivity disorder (Helmlinger, Tora, and Devys 2006; Dela Peña *et al.* 2019; Cornelio-Parra et al. 2021). On the other hand, the loss of ataxin-7 in flies is found to cause death at prepupation, but only a small number escapes death with having lesions in neuronal as well as retinal structures (Mohan, Dialynas, *et al.* 2014; Niewiadomska-Cimicka and Trottier 2019). Also, inactivation/lack of ataxin-7 causes ocular coloboma and elevation of hedgehog signaling in the forebrain in zebrafish (Carrillo-Rosas *et al.* 2019; Niewiadomska-Cimicka and Trottier 2019). Thus, the ataxin-7 subunit of SAGA plays important cellular functions, and its upregulation or downregulation is associated with various diseases.

Since alteration of ataxin-7 abundance is associated with various diseases, it is important to know the factors/mechanisms that change the cellular level of ataxin-7 toward understanding the disease pathogenesis and therapeutic interventions. However, the regulation of Sgf73/ataxin-7 is poorly understood. In view of this, we have carried out experiments to understand the regulation of Sgf73/ataxin-7 in yeast and human cells. Our results in yeast reveal that Sgf73 undergoes ubiquitylation and 26S proteasomal degradation, thus unveiling a novel ubiquitin–proteasome system (UPS) regulation of Sgf73. Alteration of such regulation changes Sgf73 abundance that affects the PIC formation and transcription. Thus, UPS fine-tunes Sgf73 in orchestrating the PIC formation and transcription. Therefore, our results reveal a novel UPS regulation of Sgf73 with physiological relevance in gene expression in yeast. Likewise, we find in human cells that ataxin-7 undergoes ubiquitylation and proteasomal degradation. Alteration of such regulation changes ataxin-7's abundance that is associated with transcription aberration and cellular pathologies, thus implicating altered UPS regulation of ataxin-7 in diseases. Collectively, our results unveil a novel UPS regulation of Sgf73/ataxin-7 in yeast and human cells for normal cellular health and implicate the alteration of such regulation in diseases.

Materials and methods

Yeast strains, plasmids, and growth media

The plasmid, pFA6a-13Myc-KanMX6 (Longtine *et al.* 1998), was used for Myc epitope tagging at the C-terminal of Sgf73. The plasmid, pRS406 (Sikorski and Hieter 1989), was used in the PCR-based disruption of *SGF73*. For N-terminal HA epitope tagging at the chromosomal locus of Sgf73 with replacement of its endogenous promoters by the *GAL1* promoter, the plasmid pFA6a-KanMX6-PGAL1-3HA (Longtine *et al.* 1998) was used. The plasmid, pFA6a-3HA-His3MX6 (Longtine *et al.* 1998), was used for HA epitope tagging of Sgf73 and Ubp8 at the C-termini in their chromosomal loci. The plasmid (pUB221) expressing hexahistidine-tagged ubiquitin was obtained from the Finley laboratory (Daniel Finley, Harvard Medical School) for ubiquitylation analysis. The plasmid, pRS416 (Sikorski and Hieter 1989), was used for the growth analysis in solid synthetic complete (SC)-uracil (plus 2% dextrose or galactose) with or without 6-*a*zau*r*acil (6-AU) and *m*yco*p*henolic *a*cid (MPA).

The strain bearing temperature sensitive (ts) mutation in Rpt4 (*rpt4*-ts or sug2-13, Sc677) and its isogenic wild-type (WT) equivalent (Sc599) were obtained from the Kodadek and Johnston laboratories (Tom Kodadek and Stephen A. Johnston; UT Southwestern Medical Center) (Russell and Johnston 2001). *SGF73* was deleted in W303a to generate ASY09, using the pRS406 plasmid (Sikorski and Hieter 1989). Multiple Myc epitope tags were added at the C-terminal of *SGF73* in W303a to generate ASY03 (Shukla, Bajwa, and Bhaumik 2006). Similarly, multiple HA epitope tags were added at the C-terminal of *SGF73* in W303a to generate ARY11a. Multiple HA epitope tags were added at the C-terminal of *SGF73* in the *rpt4*-ts and WT strains to generate ARY17 and ARY16, respectively. The plasmid, pUB221, for *CUP1*-inducible expression of hexahistidine-tagged ubiquitin was transformed into the ASY03 to generate ARY10. The endogenous promoter of *SGF73* was replaced by the *GAL1* promoter in W303a to generate the ARY09b strain. For 6-AU-based experiments, pRS416 plasmid was introduced into W303a and ARY09b to generate PYY31b and PYY28b strains, respectively. For MPA-based experiments, pRS416 plasmid was introduced into ARY11a and ARY09b to generate RCY05 and RCY06, respectively. Multiple Myc epitope tags were added at the C-terminal of *SGF73* in its chromosomal locus in the GDY28 strain (that has HA-tagged Sub2 with null mutation of *PDR5*) to generate ARY05. Similarly, multiple HA epitope tags were added at the C-termini of *SGF73 and UBP8* in a strain bearing *PDR5* null mutation in BY4741 (obtained from Dharmacon) to generate PYY86b and PYY91b strains, respectively. The ASY4 and ASY10 strains were generated by multiple Myc epitope tagging of Ubp8 and Spt20 at their C-termini at the chromosomal loci, respectively, in W303a (Shukla, Bajwa, and Bhaumik 2006; Shukla, Stanojevic, et al. 2006). The PYY99b and PYY100b strains were generated by replacing the endogenous *SGF73* promoters in the ASY4 (Ubp8-Myc; Shukla, Stanojevic, *et al.* 2006) and ASY10 (Spt20-Myc; Shukla, Bajwa, and Bhaumik 2006) strains, respectively, by the *GAL1* promoter with multiple HA epitope tagging at the N-terminal of Sgf73. The PYY97b and PYY98b strains were generated by HA epitope tagging at the C-terminal of Sgf73 at the endogenous locus in the ASY4 and ASY10 strains, respectively. The W303-1a strain that contains ~8-kb-long YLR454W *o*pen reading *f*rame (ORF) under the control of *GAL1* promoter was obtained from the Struhl laboratory (Harvard Medical School; Mason and Struhl 2005). The strain, RCY07b, was generated by replacing the endogenous *SGF73* promoter in W303-1a by the *GAL1* promoter with multiple HA epitope tagging at the N-terminal of Sgf73.

The yeast strains were grown in YPD (yeast extract *p*eptone plus 2% *d*extrose) up to an OD_{600} of 1.0 at 30°C prior to formaldehyde-based in vivo cross-linking or harvesting for RNA analysis for the studies at the ADH1, PGK1, and PYK1 genes. For ubiquitylation analysis, yeast cells were grown in SC medium (yeast nitrogen base and complete amino acid mixture plus 2% dextrose) at 30°C up to an OD_{600} of 0.7 and then treated with 250 mM of $CuSO_4$ for 6 h. The WT and *rpt4*-ts mutant strains were grown at 23°C up to an OD_{600} of 0.85 and then switched to 39°C for 1 h prior to harvesting. For Sgf73 underexpression, the yeast strain expressing Sgf73 under the control of the *GAL1*

promoter was initially grown in YPG (yeast extract peptone plus 2% galactose) at 30°C to an OD_{600} of 0.6 and then transferred to YPD for 2 and 4 h. For Sgf73 overexpression, the yeast strain expressing Sgf73 under the control of the *GAL1* promoter was grown in YPG at 30°C. To look for the abundance of Sgf73 in the presence and absence of MG132, yeast cells with null mutation of *PDR5* were grown in YPD at 30°C to an OD_{600} of 0.7 and were then treated with MG132 (75 μM) for 2 h prior to harvesting. For growth curve analysis in YPD, yeast cells were grown in YPD at 30°C to an OD_{600} of 0.1, and then the OD_{600} was measured at different time points. For analysis of the last wave of RNA polymerase II, yeast strains with the ~8-kb-long YLR454W ORF or coding sequence (under the control of the *GAL1* promoter) expressing Sgf73 under its own promoter or *GAL1* promoter were grown in YPG up to an OD_{600} of 1.0 and then switched to YPD for 1.5, 3, 4.5, and 6 min prior to formaldehyde-based in vivo cross-linking and harvesting for chromatin immunoprecipitation (ChIP) analysis.

The growth of the yeast cells was analyzed on solid SC-uracil (plus 2% dextrose or galactose) media with or without 100 μg/ml 6-AU and 15 μg/ml MPA. The yeast strain expressing Sgf73 under the *GAL1* promoter or its own endogenous promoter was transformed with a low copy number plasmid (pRS416) bearing the *URA3* gene, inoculated in liquid SC-uracil medium (with 2% dextrose or galactose), and grown up to an OD_{600} of 0.2 at 30°C. Subsequently, yeast cells were suspended in fresh liquid SC-uracil medium (with 2% dextrose or galactose) and grown up to an OD_{600} of 0.4 prior to spotting (3 μl) on solid SC-uracil medium (plus 2% dextrose or galactose) with or without 100 μg/ml 6-AU and 15 μg/ml MPA. Yeast cells were spotted with 10-fold serial dilutions, grown at 30°C, and photographed after 2 or 3 days.

WCE preparation and western blot analysis

To analyze the protein levels, yeast cells were grown in 25-ml YPD to an OD_{600} of 1.0. Yeast cells were then harvested and lysed to prepare whole-cell extract (WCE), as described for the ChIP assay. The WCE was run on an sodium dodecyl sulfate (SDS)-polyacrylamide gel and then analyzed by western blot (WB) assay. The bands in the X-ray films with short exposures using diluted protein samples were scanned and quantitated by the National Institutes of Health Image 1.62 program.

Yeast RNA isolation and RT-PCR

Total RNA was prepared from yeast cell culture following the standard protocol as described previously (Durairaj, Lahudkar, and Bhaumik 2014). Briefly, 10-ml yeast culture of an OD_{600} of 1.0 in YPD was harvested, suspended in 100-μl RNA preparation buffer (500 mM NaCl, 200 mM Tris–HCl, 100 mM Na_2EDTA, and 1% SDS) along with 100-μl phenol/chloroform/isoamyl alcohol and 100-μl volume equivalent of glass beads (acid washed; Sigma), and vortexed with a maximum speed (10 in a VWR mini-vortexer; cat. no. 58816-121) 5 times (30 s each). Subsequently, 150-μl RNA preparation buffer and 150-μl phenol/chloroform/isoamyl alcohol were added to the yeast cell suspension followed by vortexing for 15 s. The aqueous phase was collected for isolation of RNA via precipitation by ethanol.

Reverse transcriptase PCR (RT-PCR) analysis was performed according to the standard protocols, as described previously (Durairaj, Lahudkar, and Bhaumik 2014). Briefly, about 10 μg of total RNA was used in the reverse transcription assay. RNA was treated with RNase-free DNase (M610A, Promega) and then reverse-transcribed to cDNA using oligo(dT). PCR was performed using synthesized first strand as template and the primer pairs targeted to the ORFs of *ADH1*, *PYK1*, *PGK1*, *SGF73*, *ACT1*, and 18S rDNA. RT-PCR products were separated by 2.2% agarose gel electrophoresis and visualized by ethidium bromide staining. The average signal of the 3 biologically independent RT-PCR experiments is reported with standard deviation (SD; Microsoft Excel). The Student's *t*-test (with tail = 2 and types = 3) was used to determine *P* value for statistical significance of the change in the RT-PCR signals. The changes were considered to be statistically significant at $P < 0.05$. The primer pairs used in RT-PCR are described in the Supplementary Material.

Ubiquitylation assay in yeast

The ubiquitylation assay was performed as described previously (Durairaj, Lahudkar, and Bhaumik 2014; Sen *et al.* 2016; Ferdoush *et al.* 2017). Briefly, the expression of hexahistidine-tagged ubiquitin from plasmid pUB221 was induced for 6 h by the addition of $CuSO_4$ to a final concentration of 250 mM. Cells were harvested, suspended in buffer A (6 M guanidine-HCl, 100 mM Na_2HPO_4/NaH_2PO_4 at pH 8.0, and 10 mM imidazole), and lysed by glass beads. Cell lysate was centrifuged; supernatant was collected and incubated with Ni^{2+}-NTA agarose resin (Qiagen) for 1 h at 4°C and 45 min at room temperature. Following incubation, Ni^{2+}-NTA resin was washed thrice by buffer A, thrice by buffer A/TI (1 volume of buffer A and 3 volumes of buffer TI), and once by buffer TI (25 mM Tris–HCl at pH 6.8 and 20 mM imidazole). Finally, hexahistidine-tagged ubiquitin/ubiquitylated proteins were eluted by heating for 5 min at 95°C with 2× SDS-polyacrylamide gel loading buffer containing 200 mM imidazole and analyzed by WB assay.

ChIP assay in yeast

The ChIP assay for TBP and RNA polymerase II was performed as described previously (Bhaumik and Green 2003; Shukla, Bajwa, and Bhaumik 2006; Shukla, Stanojevic, et al. 2006). Briefly, yeast cells were treated with 1% formaldehyde for 15 min, quenched by glycine, collected, and suspended in lysis buffer. Following sonication, cell lysate (400-μl lysate from 50-ml yeast culture) was precleared by centrifugation, and then 100-μl lysate was used for each immunoprecipitation. Anti-TBP (obtained from the Green laboratory; Li *et al.* 2000; Bhaumik and Green 2001, 2002) and anti-Rpb1 (8WG16; Biolegend) antibodies against TBP and unphosphorylated Rpb1, respectively, were used for immunoprecipitation. Immunoprecipitated protein–DNA complexes were treated with proteinase K, the cross-links were reversed, and DNA was purified. Immunoprecipitated DNA was dissolved in 20-μl TE 8.0 (10 mM Tris–HCl and 1 mM EDTA, pH 8.0) of which 1 μl was used for PCR analysis (a total of 23 cycles). As a control, "input" DNA was isolated from 5 μl of lysate without going through the immunoprecipitation step and suspended in 100 μl of TE 8.0 to be used for PCR analysis. The PCR reactions contained [α-32P] dATP (2.5 μCi for each 25-μl reaction), and the PCR products were detected by autoradiography after separation on a 6% polyacrylamide gel. Serial dilutions of input and immunoprecipitated DNA samples were used to assess the linear range of PCR amplification. For analysis of Spt20, Sgf73, and Ubp8, we have employed modified ChIP assay, as done previously (Shukla, Bajwa, and Bhaumik 2006; Shukla, Stanojevic, et al. 2006). The primer pairs used for PCR analysis are described in the Supplementary Material.

Autoradiograms were scanned and quantitated by the National Institutes of Health Image 1.62 program. Immunoprecipitated DNAs were quantitated as the ratio of immunoprecipitate to input. Results of the biologically independent experiments are reported with SD (Microsoft Excel). The Student's *t*-test (with

tail = 2 and types = 3) was used to determine P value for statistical significance of the change in the ChIP signals. The changes were considered to be statistically significant at $P < 0.05$.

Cell line, plasmid, growth media, and transfection

Human embryonic kidney cell line, HEK293T, from American Type Culture Collection (ATCC) was used in this study. The plasmid expressing HA-tagged ubiquitin (HA-Ub) was obtained from Manas Santra (National Centre for Cell Science, Pune, India) (Malonia *et al.* 2015) for this study. HEK293T cells were grown in Dulbecco's modified Eagle medium (DMEM; HyClone) supplemented with 10% fetal bovine serum (FBS; HyClone) and penicillin (100 U/ml)–streptomycin (100 μg/ml) antibiotics (Corning) in a humidified CO_2 incubator at 37°C according to the standard protocols. Cells were subcultured using trypsin according to the standard procedures. To maintain the culture, cells were split when they reached 80% confluency by treating with trypsin-EDTA (0.25 and 0.01%, respectively). The plasmid expressing HA-Ub was transfected into HEK293T cells, using calcium phosphate method according to the standard protocols. At 24-h posttransfection, the growth medium was replaced with fresh medium. Cells were harvested at 48 h following transfection.

Proteasomal inhibition analysis in human cells

For inhibition of the proteolytic function of the 26S proteasome, cells were grown to 80% confluency and subsequently treated with MG132 or an equivalent volume of DMSO at 37°C. To harvest cells, growth medium was discarded, and cells were washed twice with ice-cold phosphate-buffered saline (PBS) (137 mM NaCl, 2.7 mM KCl, 10 mM Na_2HPO_4, and 1.8 mM KH_2PO_4 at pH 7.4). Finally, cells were scraped in PBS and centrifuged at 6,000*g* for 2 min at 4°C. The cell pellet was then lysed in radioimmunoprecipitation assay (RIPA) buffer (50 mM Tris–HCl at pH 8.0, 150 mM NaCl, 0.1% SDS, 0.5% Na-deoxycholate, 1% NP-40, and 1 mM EDTA) supplemented with protease inhibitors (complete protease inhibitor; Roche Diagnostics) and dithiothreitol (DTT) (1 mM). Following a 30-min incubation in ice with intermittent vortexing (10 s, every 10 min), cell suspension was sonicated for 30 s at an amplitude of 40 for 10-s pulses (with incubation in ice for 2 m between pulses) using a Misonix S-4000 sonicator, and then the clear supernatant was collected after centrifugation at 6,000*g* for 30 min at 4°C. Protein extracts were resolved on SDS-polyacrylamide gel and then transferred to polyvinylidene difluoride (PVDF) membrane. Subsequently, membrane was blocked in 5% nonfat milk in Tris-buffered saline [TBST (10 mM Tris–HCl at pH 7.4 and 0.9% NaCl) plus 0.1% (vol/vol) Tween 20] for at least an hour and then incubated with the primary antibody overnight at 4°C. Membrane was then washed with TBST 3 times prior to incubation with the secondary antibody conjugated with horseradish peroxidase (HRP) at room temperature for 2 h. Membrane was then washed again 3 times with TBST. The signal was detected with an ECL-Prime chemiluminescence substrate (Amersham) on an autoradiogram.

RNA isolation from human cells and real-time PCR

Total RNA isolation was performed using RiboZol RNA extraction reagent (VWR) according to the manufacturer's protocol. Following treatment with DNase (Promega), 2 μg of total RNA was reverse transcribed, as described previously (Kaja *et al.* 2021). Briefly, reverse transcription was performed using oligo(dT) as described in the protocol supplied by Promega (A3800). Such generated first strand cDNA was used for quantitative PCR (qPCR or real-time PCR) amplification (Applied Biosystems) with SYBR green PCR master mix (Applied Biosystems). Samples with no reverse transcriptase were included for each RNA sample. The relative fold expression changes were calculated using the comparative threshold cycle (C_T) method (Applied Biosystems). SDs of the means of the (Δ)C_T values were calculated from at least 3 independent RNA samples. For measurements of relative gene expression, a fold change was calculated for each sample pair and then normalized to the fold change observed for hypoxanthine phosphoribosyltransferase 1 (*HPRT1*). Primers used for PCR in human cells are as follows: 5′-TGA CACTGGCAAAACAATGCA-3′ and 5′-GGTCCTTTTCACCAGCAAG CT-3′ for *HPRT1*, and 5′-CTGCCTGTCAACTCCCACGG-3′ and 5′-CCTGGGATGGTGCCTGTGTG-3′ for *ATXN7*.

Ubiquitylation assay in human cells

For the ubiquitylation analysis, cells were transfected with either HA-Ub or an empty plasmid (pcDNA3.1 V5/His). Five micrograms of the plasmid was used for transfection in HEK293T cells. After 42 h, cells were treated with 5 μM MG132 for 6 h and harvested at 48 h. Cells were washed in chilled PBS, harvested, and lysed in RIPA buffer with 10 mM *N*-ethylmaleimide (Sigma-Aldrich) and protease inhibitors (Roche Diagnostics). The lysate was vortexed for 10 s and placed in ice for 10 min (vortexing a total of 3 times). The lysate was then sonicated for 30 s (3 cycles of 10 s each) at an amplitude of 40. The sonicated lysate was spun down at 16,000*g* at 4°C for 30 min. The supernatant was collected, and 1 mg of the total protein was used for immunoprecipitation with an anti-ataxin-7 antibody. Prior to immunoprecipitation, the extract was precleared with protein A agarose beads at 4°C for 30 min. Two micrograms of antibody was used for each immunoprecipitation overnight, followed by incubation with equilibrated protein A agarose beads. Immunoprecipitation was carried out in the presence of 300 mM NaCl in RIPA buffer, and agarose beads were washed 5 times. The first wash was done using RIPA buffer containing 300 mM NaCl, and subsequently, the second and third washes were done using FA lysis buffer (50 mM HEPES at pH 7.5, 140 mM NaCl, 1 mM EDTA, 1% Triton X-100, and 0.1% Na-deoxycholate) with 1 M NaCl, the 4th wash was done using FA-W3 buffer (10 mM Tris–HCl at pH 8.0, 0.25 M LiCl, 0.5% NP-40, 0.5% sodium deoxycholate, and 1 mM EDTA), and the last wash was done using RIPA buffer with 150 mM NaCl. Immunoprecipitate was eluted into 20-μl 1.5× SDS gel loading dye at 95°C for 20 min and analyzed by WB using anti-HA–HRP or anti-ataxin-7 antibodies.

Results

Sgf73 undergoes ubiquitylation and proteasomal degradation

Since Sgf73 has been found to interact with the 19S regulatory particle (RP) subunit of the 26S proteasome in yeast (Lee, Ezhkova, *et al.* 2005; Malik *et al.* 2009; Lee *et al.* 2011; Lim *et al.* 2013), Sgf73 may be regulated by the UPS in controlling transcription. To test this, we analyzed the stability/abundance of Sgf73 in the presence and absence of a peptide aldehyde, MG132 (carbobenzoxy-Leu-Leu-leucinal), which inhibits the proteolytic function of the proteasome. If Sgf73 is targeted for the 26S proteasomal degradation, pharmacological inhibition of the proteolytic function of the proteasome by MG132 would increase the abundance of Sgf73. However, yeast cells can be resistant to MG132, as they are capable of multidrug resistance. For this purpose, we deleted the multidrug resistance gene, *PDR5*, in the yeast strain expressing Myc-tagged Sgf73 and then analyzed the level of Myc-tagged Sgf73 with or without MG132 treatment, as done previously (Durairaj, Lahudkar, and Bhaumik 2014;

Sen *et al.* 2016; Ferdoush *et al.* 2017; Kaja *et al.* 2021). Myc epitope tagging at the C-terminal of Sgf73 at its chromosomal locus did not alter cellular growth (Fig. 1a) and transcription regulatory function of Sgf73, as the recruitment of RNA polymerase II (Rpb1; largest subunit of RNA polymerase II required for its structural and functional integrities) to the promoter of the Sgf73-regulated *GAL1* promoter (Shukla, Bajwa, and Bhaumik 2006) was not changed with Myc-tagged Sgf73 [Fig. 1b; an inactive region within chromosome V (Chr.-V) was used as a nonspecific DNA control; and the *Δsgf73* strain was used as a positive control; Shukla, Bajwa, and Bhaumik 2006]. Using Myc-epitope-tagged Sgf73 in the *PDR5* null mutant, we analyzed the level of Sgf73 following proteolytic inhibition of the proteasome by MG132. We find that the abundance of Myc-tagged Sgf73 is significantly increased following MG132 treatment (Fig. 1c and d). However, similar increased abundance of Myc-tagged Sgf73 is not observed following the treatment with DMSO (solvent that was used to prepare MG132 solution) (Fig. 1c and d). As a loading control, we analyzed the level of actin that is not regulated by the 26S proteasome (Lipford *et al.* 2005). We find that the actin level is not changed following MG132 treatment (Fig. 1c and d). Thus, our results show that the proteolytic inhibition of the proteasome by MG132 increased the level of Myc-tagged Sgf73.

Like Myc-tagged Sgf73, the abundance of HA-tagged Sgf73 is also increased in response to MG132 treatment (Fig. 1e and f). HA epitope tagging did not alter the cellular growth (Fig. 1a) or transcription regulatory activity of Sgf73 (Fig. 1b). Further, the stability of HA epitope is not regulated by the proteasome, as the abundance of HA-tagged Ubp8 (another component of SAGA's DUB module) is not increased in response to MG132 treatment (Fig. 1g and h). Therefore, our results (Fig. 1) support that 26S proteasome is involved in the degradation of Sgf73, and hence, Sgf73's abundance is increased following pharmacological inhibition of the proteolytic function of the 26S proteasome by MG132. Consistently, we observed increased abundance of Sgf73 in response to MG132 treatment following pharmacological inhibition of translation by cycloheximide (CHX) (Fig. 2a). However, such increased level of Sgf73 is not due to enhanced mRNA level of *SGF73* in response to MG132 treatment (Fig. 2b and c). Collectively, our results reveal that pharmacological inhibition of the 26S proteasome enhances the stability/abundance of Sgf73.

To complement above results genetically, we analyzed the levels of HA-tagged Sgf73 in the WT and ts mutant strains of Rpt4, an essential component of the 26S proteasome for its proteolytic activity (Rubin *et al.* 1998; Russell *et al.* 2001; Bhaumik and Malik 2008). Rpt4 is an ATPase present at the base of the 19S RP subunit of the 26S proteasome, and the ATPase activity of the base plays important role to unfold the target protein for entry into the barrel of the 20S core particle (CP) of the 26S proteasome for proteolytic degradation. If Sgf73 is degraded by the 26S proteasome, the stability/abundance of Sgf73 would be increased in the ts mutant strain of Rpt4 (also known as *sug2*-ts; Rubin *et al.* 1998; Russell *et al.* 2001) at the nonpermissive temperature. We find that the level of Sgf73 is dramatically enhanced in the *rpt4*-ts mutant strain (Fig. 2d and e). However, the level of actin (loading control) is not similarly increased in the *rpt4*-ts mutant strain in comparison with the WT equivalent (Fig. 2d and e). Thus, Sgf73 has much higher turnover than actin, and such turnover is impaired in the *rpt4*-ts mutant strain. Therefore, our results support that the 26S proteasome is involved in the degradation of Sgf73, and hence, the stability/abundance of Sgf73 is increased in the *rpt4*-ts mutant strain. Taken together, pharmacological and genetic inhibitions of the proteolytic function of the 26S proteasome dramatically enhances the abundance/stability of Sgf73, thus demonstrating the proteasomal regulation of Sgf73.

The 26S proteasome targets protein for degradation via its interaction with ubiquitin attached to the host protein. Since Sgf73 is targeted for proteasomal degradation, it is likely to be ubiquitylated. To test this, we analyzed the ubiquitylation status of Sgf73, using Ni^{2+}-NTA–based ubiquitylation assay, as done in our previous studies (Durairaj, Lahudkar, and Bhaumik 2014; Sen *et al.* 2016; Ferdoush *et al.* 2017). In this direction, we introduced a plasmid expressing hexahistidine-tagged ubiquitin under the *CUP1* promoter (that is induced in the presence of Cu^{2+}) in the yeast strain expressing Myc-tagged Sgf73. Using this strain, we performed the ubiquitylation assay, as described previously (Durairaj, Lahudkar, and Bhaumik 2014; Sen *et al.* 2016; Ferdoush *et al.* 2017). Ubiquitin and ubiquitylated proteins were precipitated from the WCE, using Ni^{2+}-NTA agarose beads that bind to the hexahistidine tag attached to ubiquitin. The precipitate was analyzed by WB assay for the presence of Sgf73 using an anti-Myc antibody against the Myc-tagged Sgf73. We observed Sgf73 in the precipitate (Fig. 2f), thus supporting the ubiquitylation of Sgf73. As a control, we performed similar experiments using the yeast strain that did not have the plasmid expressing hexahistidine-tagged ubiquitin (but expressed Myc-tagged Sgf73) and did not find Sgf73 in the precipitate (Fig. 2f). Thus, our results support that Sgf73 is ubiquitylated, and hence, Ni^{2+}-NTA agarose bead pulled down Sgf73 via its interaction with hexahistidine-tagged ubiquitin covalently attached to Sgf73.

Increased abundance of Sgf73 enhances TBP association with promoter

Our above results demonstrate that Sgf73 undergoes ubiquitylation and proteasomal degradation. In the absence of such proteasomal degradation, Sgf73's abundance/stability would be increased, as observed following pharmacological and genetic inhibitions of the proteolytic function of the 26S proteasome (Figs. 1c–f and 2d and e). Since Sgf73 regulates the PIC formation at the SAGA–regulated genes (Shukla, Bajwa, and Bhaumik 2006), increased abundance of Sgf73 in the absence of its proteasomal degradation may have an effect on the PIC formation and hence transcription. To test this, we analyzed the effect of high abundance of Sgf73 on the PIC formation at the promoters of the Sgf73/SAGA–regulated genes such as *ADH1*, *PGK1*, and *PYK1* (Holstege *et al.* 1998; Bhaumik and Green 2002; Huisinga and Pugh 2004). For this purpose, we replaced the endogenous promoter of *SGF73* by a galactose-inducible *GAL1* promoter (that is repressed in dextrose-containing growth medium but induced in galactose-containing medium; Bhaumik and Green 2001; Bhaumik *et al.* 2004) and then overexpressed *SGF73* in galactose-containing growth medium (Fig. 3a and b). Subsequently, we analyzed the recruitment of TBP (as it nucleates the PIC formation) to the promoters of *ADH1*, *PGK1*, and *PYK1*, using the ChIP assay. Our ChIP analysis revealed that the association of TBP with the promoters of *ADH1*, *PGK1*, and *PYK1* was increased in the presence of high abundance of Sgf73 (Fig. 3c–e). Such enhanced TBP association is not due to increase in global level of TBP (Fig. 3f). Moreover, the targeted recruitment of a DNA-binding protein is not correlated with its global level (e.g. TBP is not found to be recruited to the promoter in the absence of activator or coactivator, even with its high global level; Li *et al.* 2000; Bhaumik and Green 2002). Further, when yeast strain expressing Sgf73 under its own promoter (P_{SGF73}*SGF73*) was grown under similar growth conditions (Fig. 3b), the association of TBP with the promoters of these genes was not found to be increased (Fig. 3c–e). These results

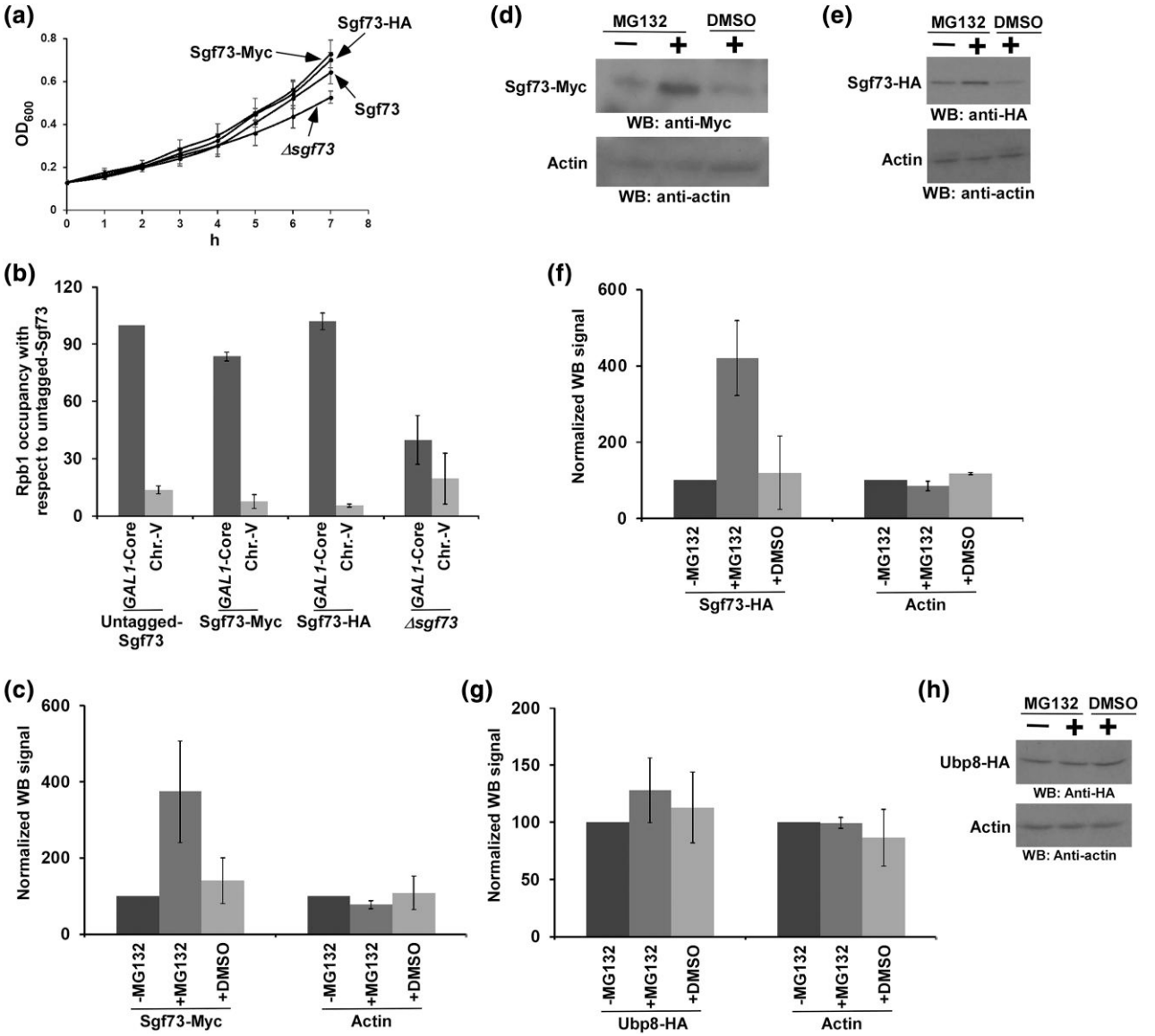

Fig. 1. Sgf73's abundance is increased following pharmacological inhibition of the proteasome. a) Growth analysis of yeast cells expressing Myc epitope-tagged Sgf73, HA epitope-tagged Sgf73, Sgf73, or with *SGF73* null mutation in liquid YPD (yeast extract *p*eptone plus 2% *d*extrose) growth medium at 30°C. b) ChIP analysis of Rpb1 association with the *GAL1* promoter in yeast strains expressing Myc/HA epitope-tagged and epitope-untagged Sgf73 or with *SGF73* null mutation. An inactive region within Chr.-V was used as a non-specific DNA control. An anti-Rpb1 antibody (8WG16; Biolegend) was used against the unphosphorylated form of the largest subunit (Rpb1) of RNA polymerase II for immunoprecipitation. c and d) Western blot (WB) analysis of Sgf73's abundance in the presence and absence of MG132 in the yeast strain expressing Myc epitope-tagged Sgf73. Yeast strain with a null mutation of *PDR5* was grown in YPD at 30°C to an OD_{600} of 0.7 and then treated with MG132 (75 μM) for 2 h prior to harvesting. Anti-Myc (9E10; Santacruz Biotechnology, Inc.) and anti-actin (A2066; Sigma) were used as primary antibodies against Myc-tagged Sgf73 and actin, respectively, in the WB analysis. e and f) WB analysis of Sgf73's abundance in the presence and absence of MG132 in the yeast strain expressing HA epitope-tagged Sgf73. An anti-HA (F-7; Santa Cruz Biotechnology, Inc.) was used as a primary antibody in the WB analysis. g and h) WB analysis of Ubp8's abundance in the presence and absence of MG132 in the yeast strain expressing HA epitope-tagged Sgf73.

demonstrate that increased abundance of Sgf73 enhances TBP association with the promoter (and hence PIC formation).

Increased abundance of Sgf73 impairs transcription elongation

Since TBP nucleates the PIC formation at the promoter and RNA polymerase II joins the PIC toward the end, the recruitment of RNA polymerase II to the promoter is likely to be increased in the presence of increased abundance of Sgf73. To test this, we analyzed the association of RNA polymerase II with the SAGA–regulated *ADH1* core promoter in response to increased abundance of Sgf73. The largest subunit of RNA polymerase II, Rpb1, served as a representative component for ChIP analysis of RNA polymerase II. Our ChIP analysis revealed that the association of RNA polymerase II with the *ADH1* promoter was increased in the presence of high abundance of Sgf73 (Fig. 4a; Supplementary Figs. 1 and 2), similar to the increased association of TBP (Fig. 3c), when compared with the yeast strain expressing Sgf73 from its own promoter (that does not overexpress Sgf73 in galactose-containing growth medium; Fig. 3b). However, the association of RNA polymerase II with the 3′-end of the *ADH1* ORF (3′ORF) is decreased in the presence of high abundance of Sgf73 (Fig. 4b; and Supplementary Figs. 1a and c and 3), but its global level was not changed (Fig. 4c). In contrast, we observed increased association of RNA polymerase II toward

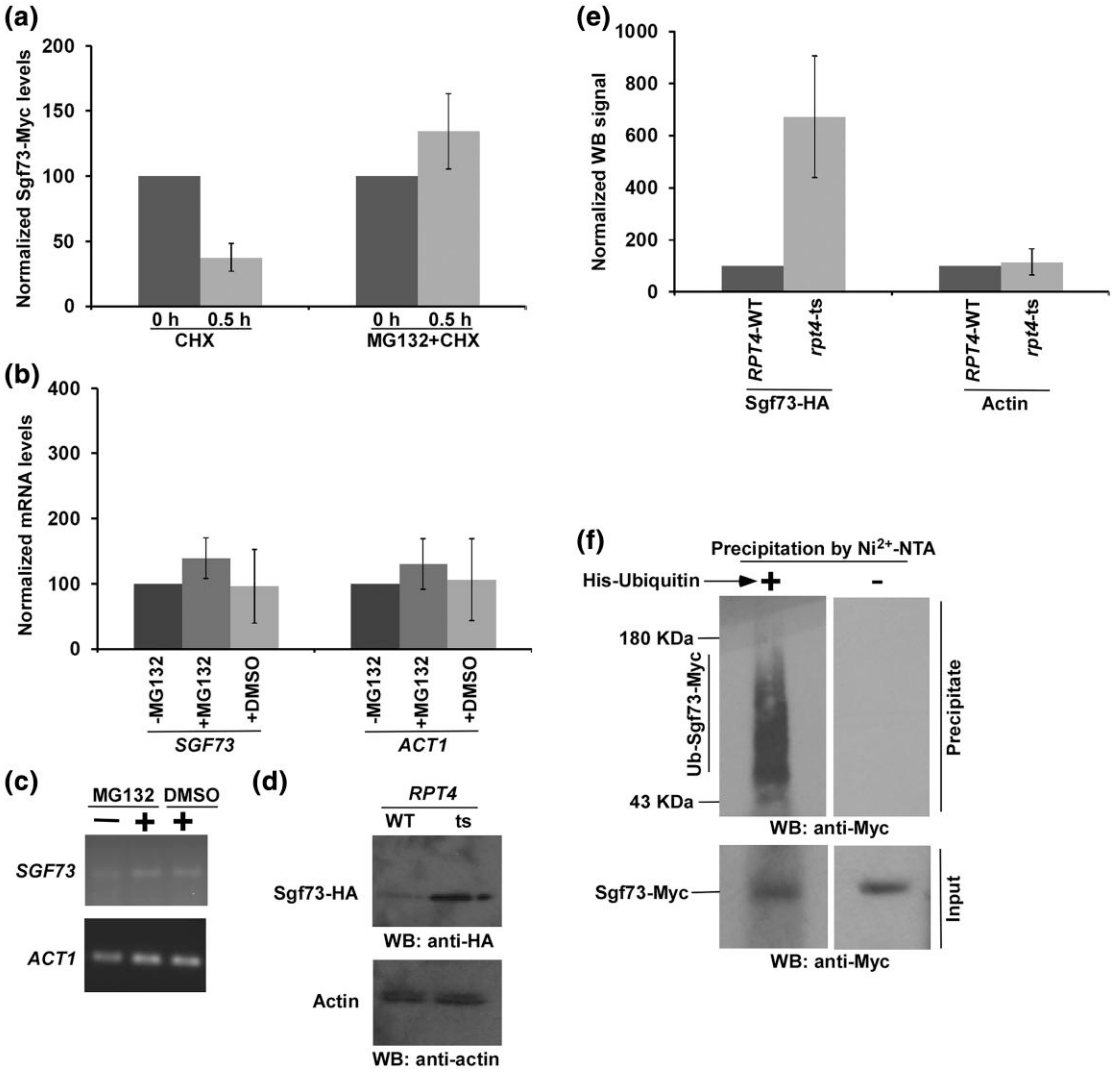

Fig. 2. Analysis of Sgf73's abundance following inhibition of translation and genetic inhibition of the proteasome and its ubiquitylation. a) WB analysis of Sgf73's abundance in the presence and absence of translational inhibitor, CHX (75 μg/ml), alone or both CHX (75 μg/ml) and MG132 (75 μM). Yeast strain with a null mutation of *PDR5* was grown in YPD at 30°C to an OD_{600} of 0.7 and then treated with CHX or both CHX and MG132 for 0.5 h prior to harvesting. b and c) RT-PCR analysis of *SGF73* and *ACT1* mRNA levels in response to MG132 treatment. Cells were grown as in Fig. 1c. d and e) WB analysis of Sgf73's abundance in the *rpt4*-ts mutant and WT strains. Both the WT and ts mutant strains expressing HA-tagged Sgf73 were grown in YPD at 23°C to an OD_{600} of 0.85 and then switched to 39°C for 1 h before harvesting for WB analysis. f) Ubiquitylation analysis of Sgf73. Yeast strains expressing Myc-tagged Sgf73 with or without hexahistidine-tagged ubiquitin were grown in SC medium at 30°C to an OD_{600} of 0.7 and then treated with $CuSO_4$ at a final concentration of 250 mM for 6 h. Precipitation was carried out by the use of Ni^{2+}-NTA agarose beads, and WB analysis was performed using an anti-Myc antibody against Myc-tagged Sgf73.

the 5′-end of the *ADH1* ORF (regions A and B as depicted in the bottom panel of Fig. 4a) in the presence of high abundance of Sgf73 (Fig. 4d and e; Supplementary Figs. 1a and c and 3). These results indicate that RNA polymerase II is accumulated at the 5′-end of the *ADH1* ORF, and thus less RNA polymerase II was observed at the 3′-end of the ORF in the presence of increased abundance of Sgf73 (Fig. 4f). However, similar decrease in RNA polymerase II level at the *ADH1* 3′ORF was not observed in the WT strain expressing Sgf73 from its own promoter (Fig. 4f). These observations indicate that increased abundance of Sgf73 impairs transcription elongation. Consistently, we also observed decreased level of RNA polymerase II at the 3′-end, but not 5′-end, of the *ADH1* ORF in the presence of high abundance of Sgf73 at 120 min upon switching on the expression of Sgf73 under the *GAL1* promoter in galactose-containing growth medium (Fig. 4g–j). Further, in agreement, our analysis of the last wave of RNA polymerase II at ~8-kb-long ORF (YLR454W) under the *GAL1* promoter upon switching the carbon source in the growth medium from galactose to dextrose revealed slow movement/processivity of RNA polymerase II in the presence of high abundance of Sgf73 (Fig. 5a and b). Together, these results indicate impairment of transcription elongation in response to increased Sgf73 abundance. Consistently, increased abundance of Sgf73 decreased *ADH1* mRNA level (Fig. 5c) and reduced cellular growth in solid SC-uracil medium containing 6-AU or MPA that lowers the nucleotide pool for transcription elongation by RNA polymerase II (Fig. 5d and e).

Like *ADH1*, SAGA–regulated *PYK1* also shows decreased association of RNA polymerase II with the 3′-end of its ORF, but not with its core promoter and/or 5′-ORF in response to increased Sgf73 abundance (Fig. 6a–c). Therefore, our results demonstrate more RNA polymerase II at the 5′-end, but less at the 3′-end, of the *PYK1* ORF in the presence of increased abundance of Sgf73 (Fig. 6d). However, similar decrease in RNA polymerase II level

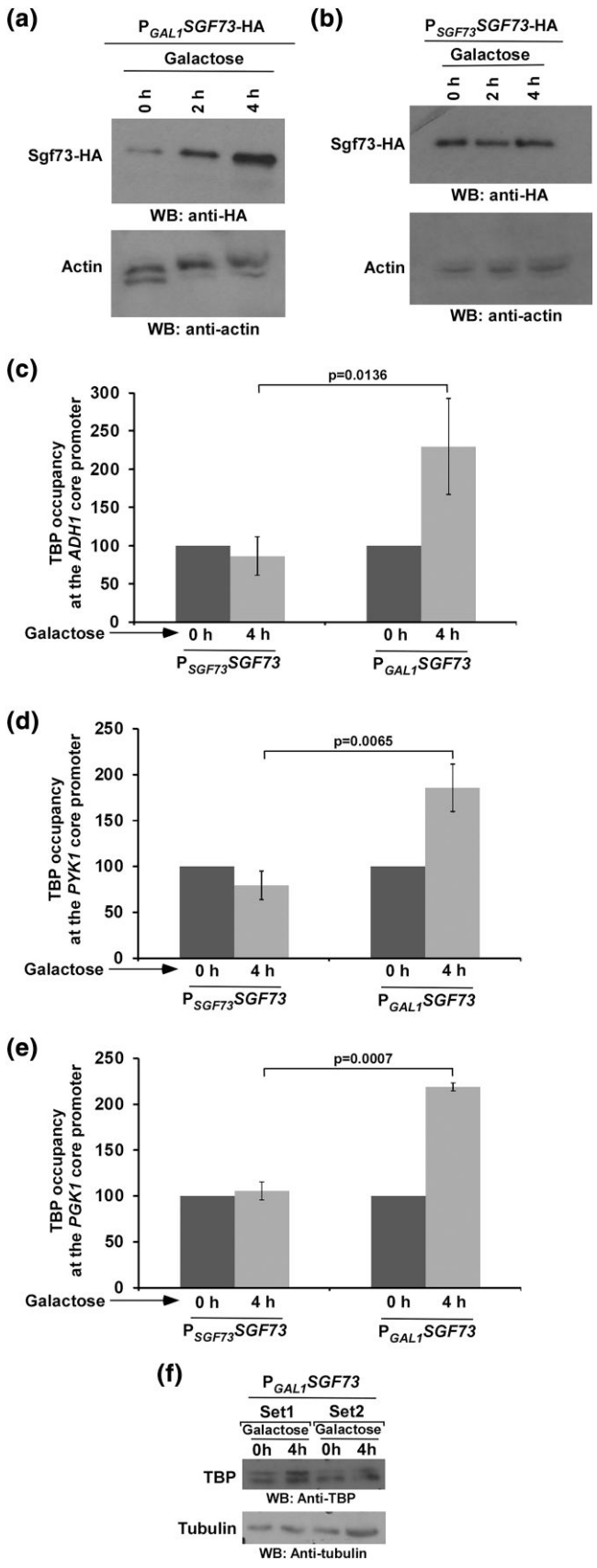

Fig. 3. Increased abundance of Sgf73 enhances TBP association with the core promoter. a) Sgf73 expression analysis under the control of *GAL1* promoter (P_{GAL1}SGF73) in galactose-containing growth medium (or YPG; yeast extract, peptone plus 2% galactose) by WB assay. Yeast cells were (continued)

at the 3′-end of the *PYK1* ORF was not observed in the yeast strain expressing Sgf73 from its own promoter (Fig. 6d). These results indicate that transcription elongation of *PYK1* is impaired in the presence of high abundance of Sgf73, leading to the accumulation of RNA polymerase II at its 5′ORF (Fig. 6b and c), consistent with slow movement of RNA polymerase II in response to increased Sgf73 level (Fig. 5a and b). Thus, *PYK1* mRNA level is decreased, when the Sgf73 abundance is increased (Fig. 6e). Similar to the results at *ADH1* and *PYK1*, we also found decreased level of RNA polymerase II at the 3′-end in comparison with the 5′-end of the *PGK1* ORF in the presence of high abundance of Sgf73 (Fig. 6f–i), indicating impairment of transcription elongation.

The decreased transcription elongation in the presence of increased abundance of Sgf73 could be mediated via altered association of Ubp8 (a key component of the DUB module of SAGA with histone H2B DUB activity; Henry *et al.* 2003; Shukla, Stanojevic, *et al.* 2006; Baker and Grant 2007; Rodriguez-Navarro 2009; Köhler *et al.* 2010; Samara *et al.* 2010; Bhaumik 2011; Lee *et al.* 2011; Samara *et al.* 2012; Spedale *et al.* 2012; Cheon *et al.* 2020) with SAGA or upstream activating sequence (UAS), as both increased and decreased histone H2B ubiquitylation or loss of Ubp8 impairs transcription elongation (Wyce *et al.* 2007). Therefore, we next analyzed the effect of the increased abundance of Sgf73 on Ubp8 recruitment to the SAGA–regulated *GAL1* UAS, using the ChIP assay in the strain expressing Myc epitope-tagged Ubp8 with and without overexpression of HA-tagged Sgf73 (Fig. 7a). We find that the recruitment of Ubp8 to the *GAL1* UAS is decreased in the presence of excess Sgf73 (Fig. 7a–c). Unlike Ubp8, the recruitment of Sgf73 to the *GAL1* UAS was not decreased following Sgf73 overexpression (Fig. 7a and b). Similarly, the recruitment of a core scaffolding component of SAGA, Spt20, to the *GAL1* UAS is not decreased in the presence of excess of Sgf73 (Fig. 7b and d). These results suggest that the association of the DUB module with the rest of SAGA is decreased in the presence of increased abundance of Sgf73, which could be associated with decrease transcription elongation, as transcription elongation is impaired in *Δubp8* (Wyce *et al.* 2007). Such DUB-depleted SAGA may be efficient in the PIC formation, as the SAGA's DUB module is located closely to its TBP–interacting surface (Wang *et al.* 2020) and could interfere with SAGA's interaction with TBP. In fact, we observed increased association of TBP with the promoter in the presence of high abundance of Sgf73 (Fig. 3c–e) that does not enhance core SAGA recruitment, but reduces DUB assembly with core SAGA (Fig. 7b).

Fig. 3. (Continued)
initially grown at 30°C to an OD_{600} of 0.4 and then were collected immediately (0 h) and after 2 and 4 h for WB analysis. b) Sgf73 expression analysis under its endogenous promoter (P_{SGF73}SGF73) in galactose-containing growth medium by WB assay. Yeast cells were grown as in a). c, d and e) ChIP analysis of the association of TBP with the core promoter regions of *ADH1*, *PYK1*, and *PGK1* in the yeast strains expressing *SGF73* under the control of the *GAL1* promoter (P_{GAL1}SGF73) or its own endogenous promoter (P_{SGF73}SGF73), using an anti-TBP antibody against TBP. Yeast cells were grown as in a) prior to formaldehyde-based in vivo cross-linking and harvesting. Immunoprecipitated DNA samples were analyzed by PCR using the primer pairs targeted to the core promoter regions of *ADH1*, *PYK1*, and *PGK1*. The ChIP signal at 4 h was normalized with respect to 0 h in each strain (i.e. P_{SGF73}SGF73- and P_{GAL1}SGF73-containing strains). Normalized ChIP signals at 4 h between these 2 strains were compared for analyzing the effect of increased abundance of Sgf73 on TBP association with the core promoter. f) The WB analysis of TBP in the yeast strain expressing Sgf73 under the *GAL1* promoter. Yeast cells were grown as in c).

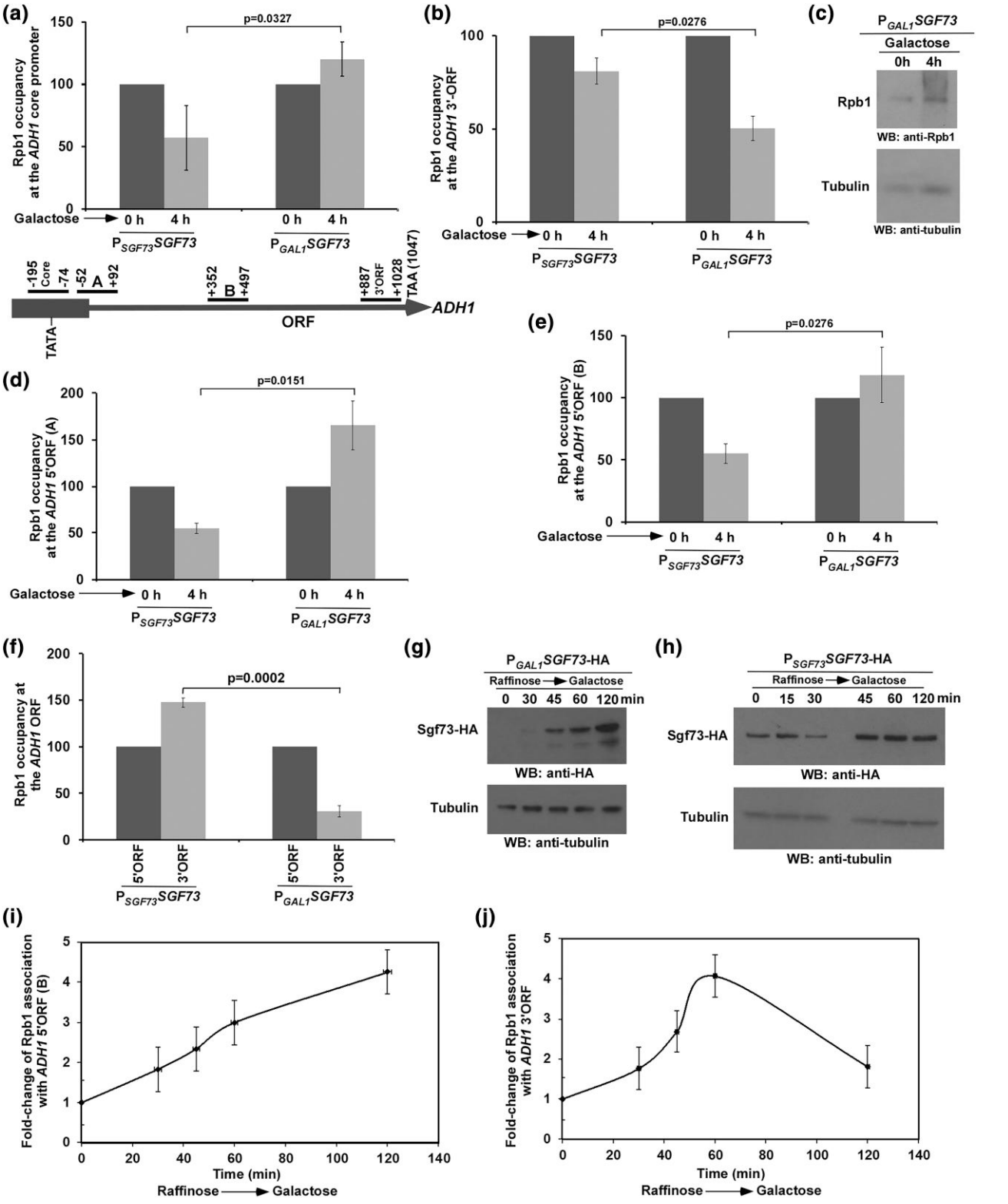

Fig. 4. Increased abundance of Sgf73 impairs transcription elongation. a and b) ChIP analysis of the association of Rpb1 with the core promoter and the 3′ end of the coding sequence (or ORF) of *ADH1* in the strains expressing *SGF73* under the control of the *GAL1* promoter (P_{GAL1}*SGF73*) or its own endogenous promoter (P_{SGF73}*SGF73*), using 8WG16 antibody (Biolegend) against the carboxy-terminal domain of Rpb1. The comparison of the ChIP signals at 0 h in these 2 strains is presented in Supplementary Figs. 1–3. The ChIP signal at 4 h was normalized with respect to 0 h in each strain (i.e. P_{SGF73}*SGF73*- and P_{GAL1}*SGF73*-containing strains). Normalized ChIP signals at 4 h between these 2 strains were compared for analyzing the effect of increased abundance of Sgf73 on Rpb1 association. The ChIP signals without normalization are presented in Supplementary Figs. 1–3. Locations of the primer pairs are schematically shown at the bottom of a) with respect to translation start site. c) The WB analysis of Rpb1 in the P_{GAL1}*SGF73*-containing strain under the growth condition as in a) and b). d and e) ChIP analysis of the association of Rpb1 with the promoter proximal region (A) and region B toward the 5′-end of the *ADH1* ORF (a) in the strains expressing *SGF73* under the control of the *GAL1* promoter (P_{GAL1}*SGF73*) or its own endogenous promoter (P_{SGF73}*SGF73*) at 4 h

(continued)

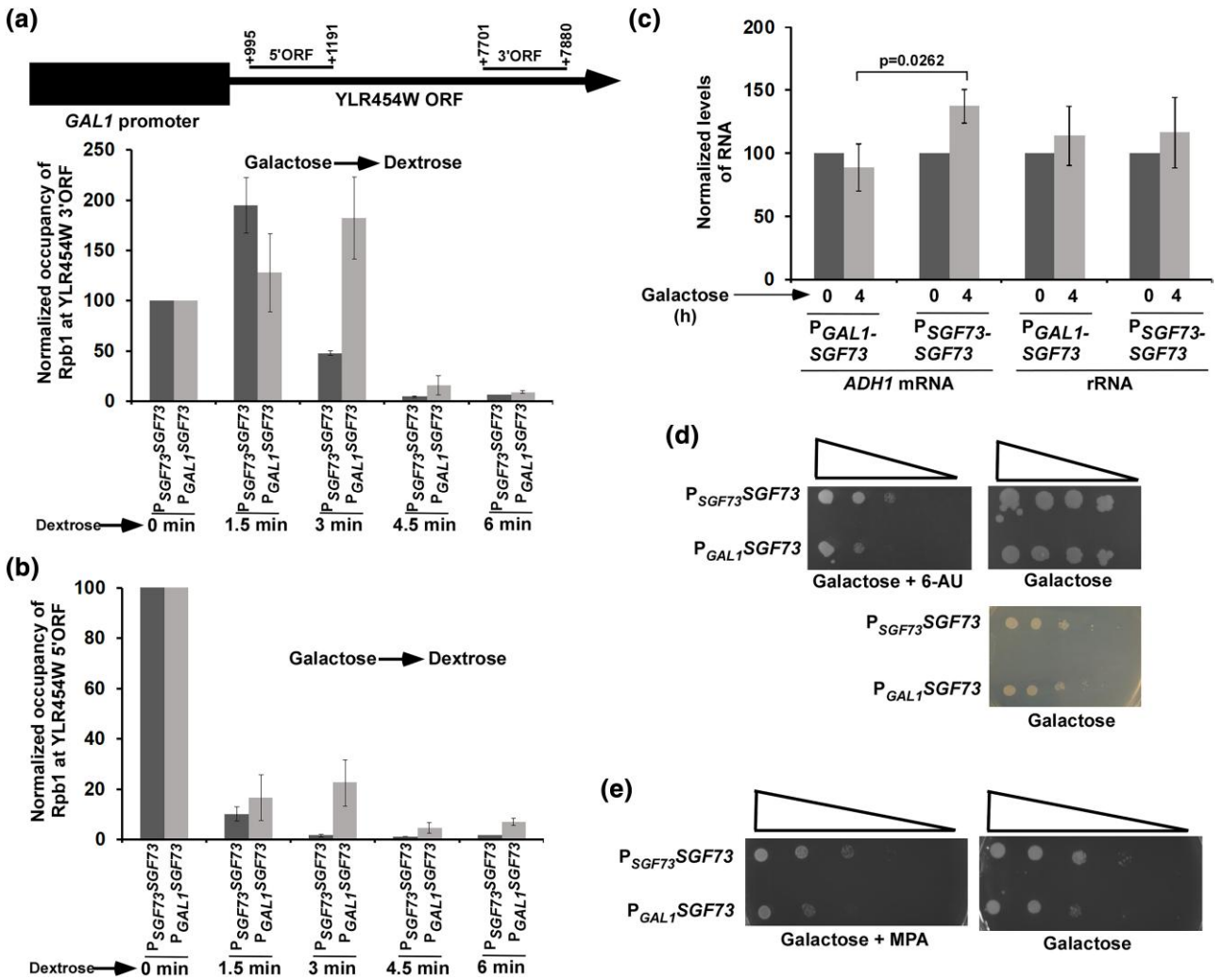

Fig. 5. Increased abundance of Sgf73 decreases movement/processivity of RNA polymerase II at the coding sequence. a and b) ChIP analysis of the association of Rpb1 with the 5′- and 3′-ends of the ~8-kb-long ORF (YDR454W) under the *GAL1* promoter upon switching the carbon source in the growth medium from galactose to dextrose. c) RT-PCR analysis of *ADH1* mRNA levels in the strains expressing *SGF73* under the control of the *GAL1* promoter or its own endogenous promoter. 18S rRNA levels were monitored as control. d) Growth analysis of the yeast strains expressing *SGF73* under the control of the *GAL1* promoter (P_{GAL1}SGF73) or its own endogenous promoter (P_{SGF73}SGF73) in the solid SC-uracil medium containing 2% galactose with or without 100 μg/ml 6-AU at 30°C. The right bottom panel is the shorter growth analysis in galactose-containing medium without 6-AU. e) Growth analysis of the yeast strains expressing *SGF73* under the *GAL1* promoter or its own endogenous promoter in the SC-uracil medium containing 2% galactose with or without 15 μg/ml MPA at 30°C.

Decreased abundance of Sgf73 impairs the PIC formation and transcription

Our above results demonstrate that Sgf73 level is increased following impairment of proteasomal degradation and increased abundance of Sgf73 enhances the association of TBP and RNA polymerase II with the promoter and decreases transcription elongation. However, increased degradation of Sgf73 (e.g. via decreased deubiquitylation or increased ubiquitylation) would lower the level of Sgf73. Since Sgf73 maintains SAGA's overall structural integrity, decreased abundance of Sgf73 would affect the PIC formation and hence transcription. To address this, we analyzed the recruitment of TBP to the *ADH1*, *PGK1*, and *PYK1* promoters after shutting down the expression of Sgf73 in dextrose-containing growth medium in the yeast strain expressing Sgf73 under the *GAL1* promoter (Fig. 8a and b). Our ChIP analysis revealed that the decreased abundance of Sgf73 lowers the recruitment of TBP to the *ADH1*, *PGK1*, and *PYK1* promoters (Fig. 8c–e) but

Fig. 4. (Continued)
in galactose, as done in the a) and b). The ChIP signals without normalization are presented in Supplementary Figs. 2, 3. f) Relative level of Rpb1 at the 3′-end with respect to the 5′-end of the *ADH1* ORF in the strains expressing *SGF73* under the control of the *GAL1* promoter (P_{GAL1}SGF73) or its own endogenous promoter (P_{SGF73}SGF73) at 4 h in galactose. g) The WB analysis of Sgf73 in the yeast strain expressing Sgf73 under the *GAL1* promoter upon switching the carbon source in the growth medium from raffinose to galactose. h) The WB analysis of Sgf73 in the yeast strain expressing Sgf73 under its own promoter upon switching the carbon source in the growth medium from raffinose to galactose. i and j) The ChIP analysis of RNA polymerase II toward the 5′- and 3′-ends of the *ADH1* ORF (5′ORF/B and 3′ORF) in the yeast strain expressing Sgf73 under its own promoter or under the *GAL1* promoter upon switching the carbon source in the growth medium from raffinose to galactose. The fold changes of the ChIP signals in the yeast strain expressing Sgf73 under the *GAL1* promoter with respect to the yeast strain expressing Sgf73 under its own promoter are plotted against the time in galactose-containing growth medium.

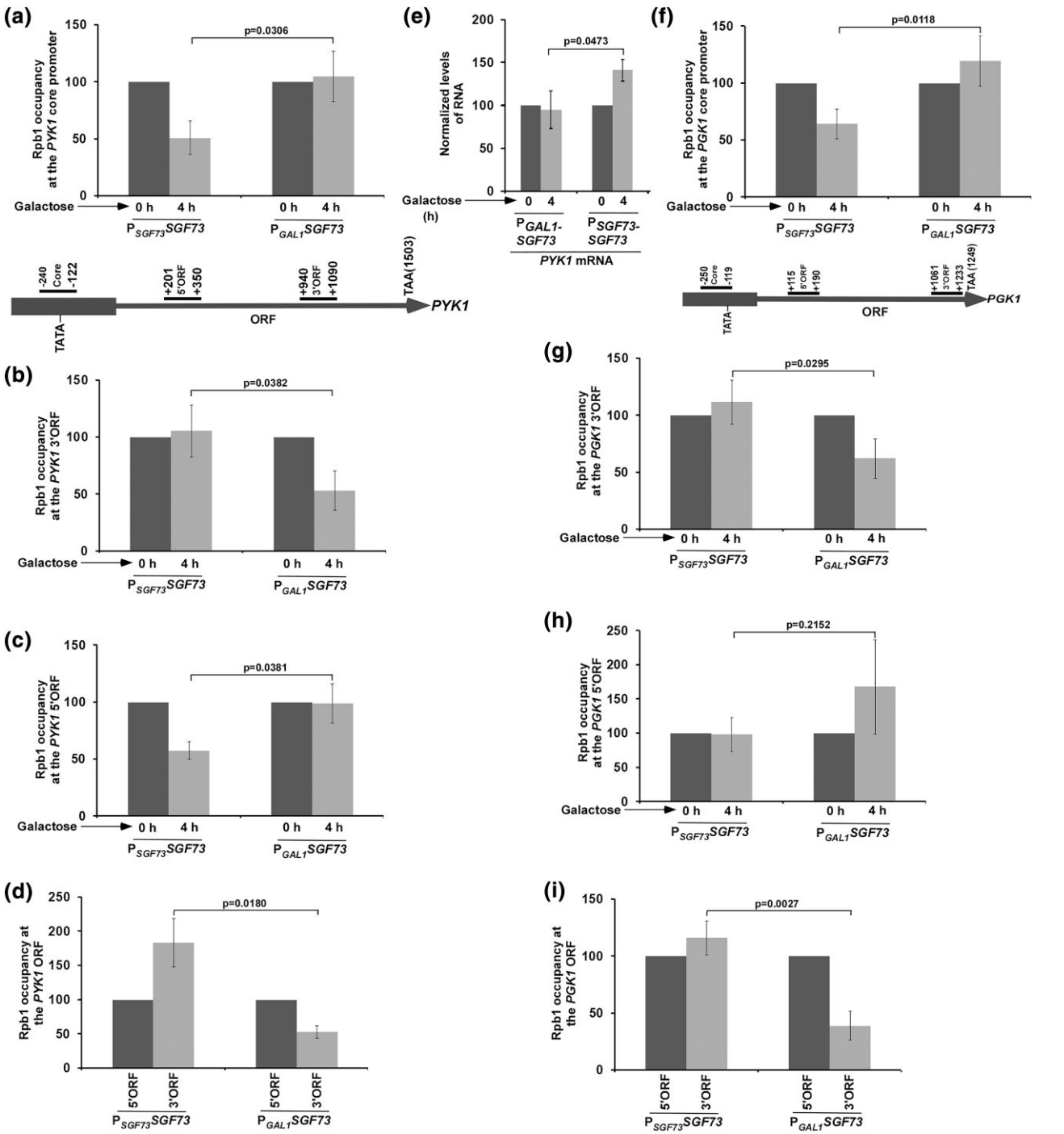

Fig. 6. Analysis of Rpb1 association with *PYK1* and *PGK1* in response to increased abundance of Sgf73. a–c) ChIP analysis of the association of Rpb1 with the promoter and ORF regions (5′ORF and 3′ORF) of *PYK1* in the yeast strains expressing *SGF73* under the control of the *GAL1* promoter (P_{GAL1}*SGF73*) or its own endogenous promoter (P_{SGF73}*SGF73*). d) Relative levels of Rpb1 at the 3′-end with respect to the 5′-end of the *PYK1* coding sequence in the strains expressing *SGF73* under the *GAL1* promoter or its own endogenous promoter at 4 h in galactose. e) RT-PCR analysis of *PYK1* mRNA levels in the strains expressing *SGF73* under the control of the *GAL1* promoter or its own endogenous promoter. 18S rRNA levels were monitored as control and are presented in Fig. 5c. f–h) ChIP analysis of the association of Rpb1 with the promoter and the coding regions (5′ORF and 3′ORF) of *PGK1* in the yeast strains expressing *SGF73* under the *GAL1* promoter or its own endogenous promoter. i) Relative levels of Rpb1 at the 3′-end with respect to the 5′-end of the *PGK1* coding sequence in the strains expressing *SGF73* under the *GAL1* promoter or its own endogenous promoter at 4 h in galactose.

not global level of TBP (Fig. 8f). Likewise, the recruitment of RNA polymerase II (Rpb1) to these promoters was also reduced (Fig. 8g–i), but not the global level of Rpb1 (Fig. 8j), when the abundance of Sgf73 was lowered (Fig. 8a and b). Thus, decreased abundance of Sgf73 impairs the PIC formation. Likewise, the levels of RNA polymerase II at the ORFs of these genes were reduced when Sgf73 level was decreased (Fig. 9a–c). Consistently, we observed reduced mRNA levels of *ADH1*, *PGK1*, and *PYK1* in response to decreased Sgf73 level (Fig. 9d and e). Thus, decreased level of Sgf73 impairs the PIC formation and transcription.

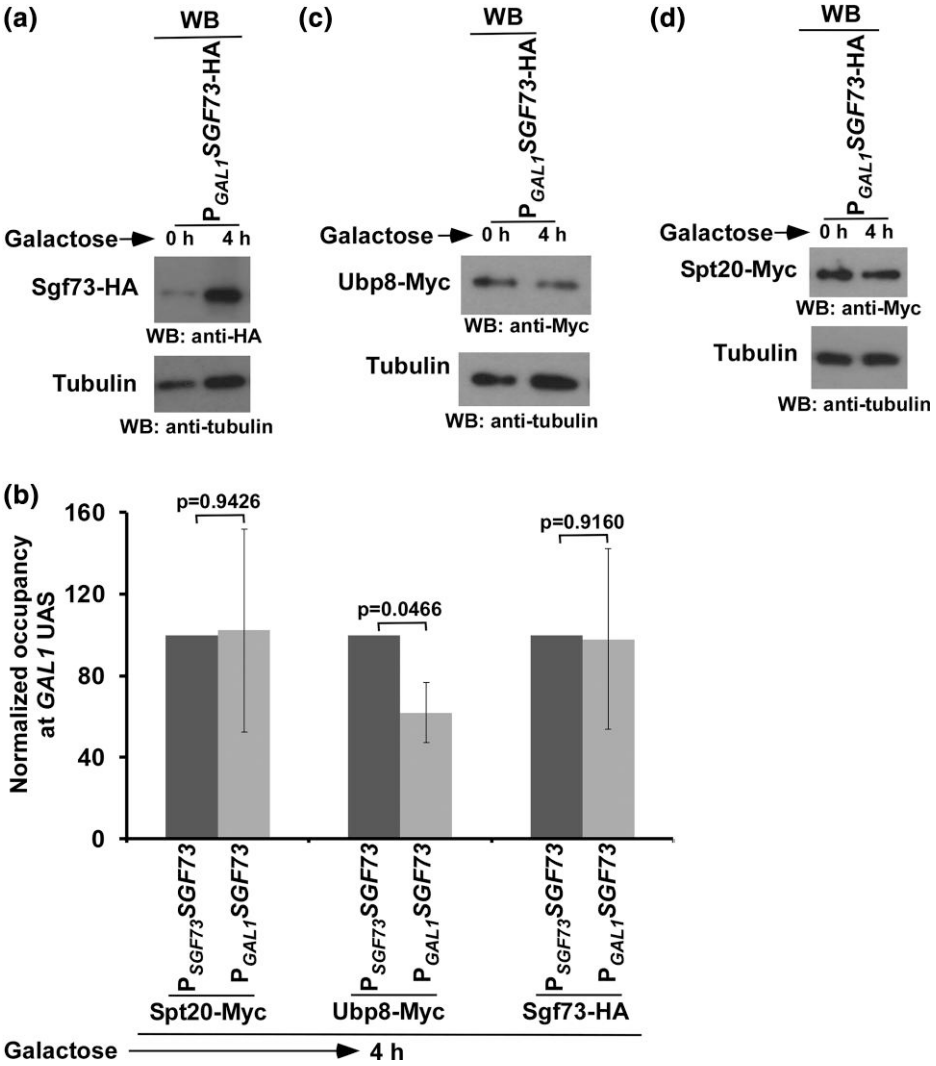

Fig. 7. Analysis of the recruitment of Spt20, Sgf73, and Ubp8 to the *GAL1* UAS in the presence of increased abundance of Sgf73. a) The WB analysis of Sgf73 in the yeast strains expressing HA-tagged Sgf73 under the inducible *GAL1* promoter (P_{GAL1}*SGF73*-HA) or its own promoter (P_{SGF73}*SGF73*-HA). Yeast cells were grown as in Fig. 3a. b) The ChIP analysis of Ubp8, Spt20, and Sgf73 at the *GAL1* UAS. Cells were grown as in a). There are 2 *GAL1* UASs in the yeast strain expressing Sgf73 under the *GAL1* promoter. For the ChIP analysis at the endogenous *GAL1* UAS, the specific primer pair that selectively amplified the endogenous *GAL1* UAS was used. The ChIP signal at 4 h was normalized with respect to 0 h in each strain. Subsequently, the ChIP signal at 4 h in the yeast strain expressing Sgf73 under its own promoter was set to 100, and the ChIP signal at 4 h in the yeast strain expressing Sgf73 under the *GAL1* promoter was normalized with respect to 100 (i.e. ChIP signal at 4 hours in the yeast strain expressing Sgf73 under its own promoter). c) The WB analysis of Myc-tagged Ubp8 in the yeast strain expressing Sgf73 under the *GAL1* promoter. d) The WB analysis of Myc-tagged Spt20 in the yeast strain expressing Sgf73 under the inducible *GAL1* promoter.

Ataxin-7 undergoes ubiquitylation and proteasomal degradation with implications in diseases

Our above results demonstrated a novel UPS regulation of Sgf73 with physiological relevance in yeast. Since Sgf73 and UPS are conserved from yeast to humans, similar UPS regulatory mechanisms are likely to exist in humans. To test this, we analyzed ubiquitylation and proteasomal degradation of Sgf73's homologue, ataxin-7, in human cells, HEK293T. We find that ataxin-7 level is increased in HEK293T cells following inhibition of the 26S proteasome by MG132 (Fig. 10a and b). However, such increase was not observed at the level of *ATXN7* mRNA (*ATXN7* is the gene for ataxin-7) following MG132 treatment (Fig. 10c). These results support proteasomal regulation of ataxin-7. Since the 26S proteasome targets ubiquitylated proteins for degradation, ataxin-7 is likely to be ubiquitylated. To test this, we introduced a plasmid expressing HA-Ub or an empty plasmid by transient transfection in HEK293T cells, grew for 42 h, and then harvested following MG132 treatment for 6 h. Subsequently, the WCE was prepared, followed by immunoprecipitation using an anti-ataxin-7 antibody. The immunoprecipitate was analyzed by WB for the presence of ubiquitylated ataxin-7 using anti-HA–HRP (that recognizes HA epitope attached to ubiquitin) and anti-ataxin-7 [that recognizes ataxin-7 as well as ubiquitylated-ataxin-7 (if exists)] antibodies. We observed ubiquitylated ataxin-7 in the immunoprecipitate (Fig. 10d). Thus, like in yeast (Figs. 1 and 2), ataxin-7 undergoes ubiquitylation and proteasomal degradation in human cells.

Alteration of UPS regulation would change the cellular abundance of ataxin-7, leading to altered transcription and cellular pathologies, as ataxin-7 maintains SAGA's integrity and DUB activity, thus controlling transcription and normal cellular

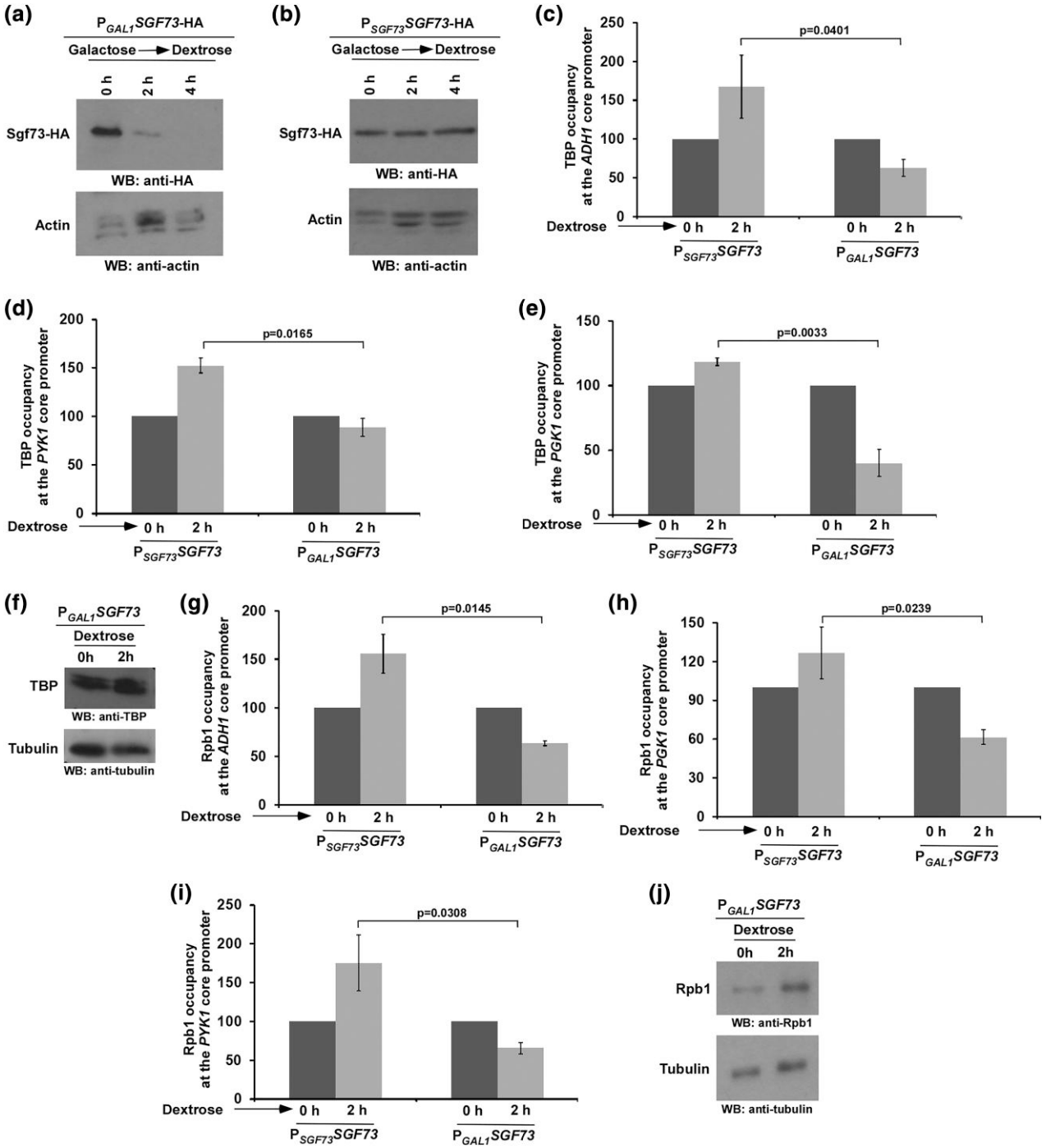

Fig. 8. Decreased abundance of Sgf73 impairs the PIC formation. a) Analysis of Sgf73 expression under the control of *GAL1* promoter in dextrose-containing growth medium by WB assay. Yeast cells were initially grown in galactose-containing medium at 30°C to an OD_{600} of 0.6 and then were collected immediately (0 h) and after switching to dextrose-containing medium at 2 and 4 h for WB analysis. b) Analysis of Sgf73 expression under its endogenous promoter in dextrose-containing growth medium by WB assay. Yeast cells were grown as in a). c–e) ChIP analysis of TBP association with the core promoter regions of *ADH1*, *PYK1*, and *PGK1* following decreased expression of Sgf73. Yeast cells expressing *SGF73* under the *GAL1* promoter or its own endogenous promoter were grown as in a) prior to formaldehyde-based in vivo cross-linking and harvesting. f) The WB analysis of TBP under the growth conditions as in the a) in the yeast strain expressing Sgf73 under the *GAL1* promoter. g–i) ChIP analysis of Rpb1 association with the core promoter regions of *ADH1*, *PYK1*, and *PGK1* following decreased expression of Sgf73 in dextrose-containing growth medium. Yeast cells were grown as in a). j) The WB analysis of Rpb1 under the growth conditions as in a) in the yeast strain expressing Sgf73 under the *GAL1* promoter.

functions (Palhan *et al.* 2005; Ström et al. 2005; Weake *et al.* 2008; Furrer *et al.* 2011; Lang *et al.* 2011; Bonnet *et al.* 2014; Ristic *et al.* 2014; Li *et al.* 2018). Indeed, transcription is found to be impaired when ataxin-7 is downregulated in HEK 293T cells (Palhan *et al.* 2005), similar to the results in yeast, and decreased ataxin-7 level caused childhood blindness, ocular coloboma, neuronal and retinal lesions, and neurodegeneration (Yanicostas *et al.* 2012; Mohan, Abmayr, and Workman 2014; Mohan, Dialynas, et al. 2014; Karam and Trottier 2018; Carrillo-Rosas *et al.* 2019; Niewiadomska-Cimicka and Trottier 2019; Guha *et al.* 2022).

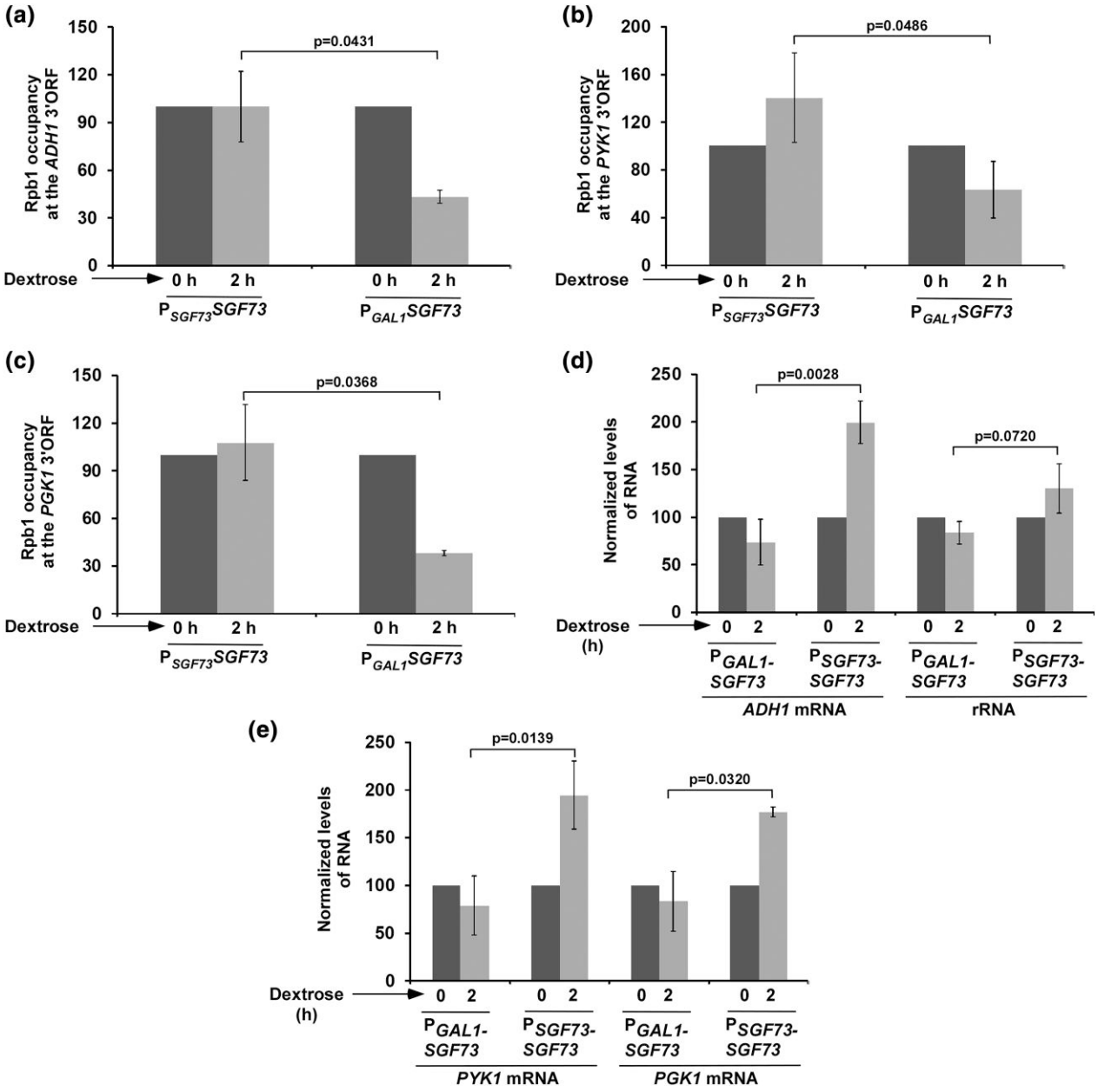

Fig. 9. Decreased abundance of Sgf73 impairs transcription. a–c) ChIP analysis of Rpb1 association with the ORFs of *ADH1*, *PYK1*, and *PGK1* following decreased expression of Sgf73 in dextrose-containing medium. Yeast cells were grown as in Fig. 8a. d) RT-PCR analysis of *ADH1* mRNA levels in the strains expressing *SGF73* under the *GAL1* promoter or its own endogenous promoter in dextrose-containing growth medium. e) RT-PCR analysis of *PYK1* and *PGK1* mRNA levels in the strains expressing *SGF73* under the *GAL1* promoter or its own endogenous promoter in dextrose-containing growth medium.

Further, like in yeast, increased ataxin-7 level is found to reduce transcription (Ström et al. 2005) and is associated with attention-deficit/hyperactivity disorder (Helmlinger, Tora, and Devys 2006; Dela Peña *et al.* 2019; Cornelio-Parra *et al.* 2021). Furthermore, our cBioPortal analysis (https://www.cbioportal.org/; Cerami *et al.* 2012; Gao *et al.* 2013; Davis *et al.* 2014) revealed that ataxin-7 is modulated via gene amplification or depletion in various cancer patient samples (Fig. 10e), indicating the association of the altered levels of ataxin-7 in cancer. However, it is unknown whether the change of ataxin-7 level in these disease states or patient samples can occur via the alteration of its proteasomal degradation. Intriguingly, our UALCAN web portal (http://ualcan.path.uab.edu/; Chandrashekar *et al.* 2017; Chen *et al.* 2019) analysis revealed that ataxin-7 is upregulated at the protein, but not mRNA, level in cancer patient samples (Fig. 10f and g). Such increased level of ataxin-7 protein could be resulted via impairment of its proteasomal degradation, which remains to be further investigated. Nonetheless, our results unveil a new UPS regulation of ataxin-7 with possible implications in diseases.

Discussion

Sgf73 plays a pivotal role in maintaining SAGA's integrity (Shukla, Bajwa, and Bhaumik 2006; Köhler *et al.* 2008; Lee *et al.* 2009; Wang *et al.* 2020) and hence PIC formation and transcription (Shukla, Bajwa, and Bhaumik 2006). Thus, Sgf73 is an important point of regulation of SAGA. However, it remains unknown how Sgf73 itself is regulated. Here, we show that Sgf73 undergoes ubiquitylation

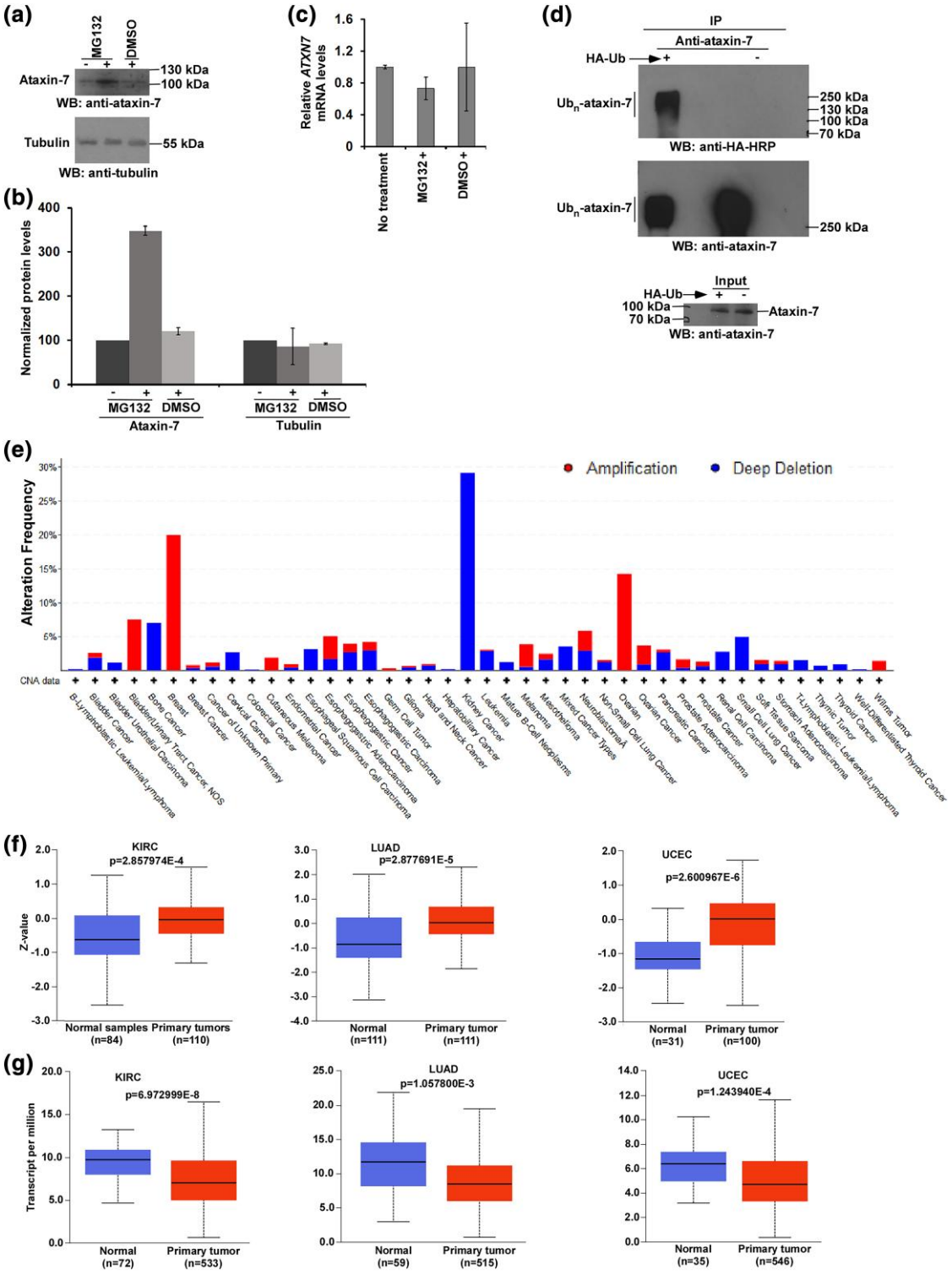

Fig. 10. Proteasomal regulation of ataxin-7/ATXN7 in HEK293T cells. a and b) Inhibition of the proteolytic activity of the 26S proteasome by 20 μM MG132 for 10 h increases the stability/abundance of ataxin-7. When cells reached 80% confluency, they were treated with MG132/DMSO for 10 h before harvesting. Proteins were extracted and analyzed by WB using anti-ataxin-7 (Catalogue no. PA1-749; Thermo Fisher Scientific) and anti-tubulin (Catalogue no. E7; Developmental Studies Hybridoma Bank) antibodies. The WB signals of ataxin-7 following 10-h treatment with MG132 and DMSO were normalized with respect to the ataxin-7 WB signal of the untreated cells. c) RNA analysis. HEK293T cells were grown to 80% confluency before treatment with 20 μM MG132 for 10 h. DMSO-treated cells were used as a control by the addition of the equal volume of DMSO as the MG132 solution. Following the treatments, RNA was isolated for cDNA synthesis. Subsequently, real-time PCR was performed to measure relative ataxin-7/ATXN7 gene (*ATXN7*) expression as described in *Materials and Methods*. d) Ubiquitylation analysis of ataxin-7 in HEK293T cells under high stringency washing conditions, as described in *Materials and Methods*. HEK293T cells were transfected with a plasmid expressing HA-Ub or an empty plasmid that does not express HA-Ub and treated with 5 μM MG132 for 6 h at 42-h posttransfection, and subsequently, the WCE was prepared for immunoprecipitation (IP) to pull down ataxin-7 using an anti-antaxin-7 antibody. Immunoprecipitates were then analyzed by WB using anti-HA–HRP and anti-ataxin-7 antibodies. +, HEK293T cells with a plasmid expressing HA-Ub; –, HEK293T cells with an empty plasmid; and Ub$_n$, polyubiquitin. e) Cross-cancer analysis of copy number alterations (CNA) in *ATXN7* based on the patient samples in the cBioPortal database. All patient samples (a total of 110,747 patients/115,399 samples from 262 studies) were

(continued)

and 26S proteasomal degradation, thus unveiling a novel regulation of Sgf73 by the UPS in controlling its abundance/stability. Increased or decreased abundance of Sgf73 alters the association of TBP and RNA polymerase II with the active genes and hence transcription. Thus, our results reveal that Sgf73 is fine-tuned by UPS in orchestrating transcription.

Transcriptionally active genes are associated with histone H2B monoubiquitylation (Xiao *et al.* 2005; Bhaumik *et al.* 2007; Shukla and Bhaumik 2007; Shukla *et al.* 2009; Sen and Bhaumik 2013; Sen *et al.* 2013) which occurs via the sequential catalytic actions of E1 ubiquitin activating enzyme, E2 ubiquitin conjugase, and E3 ubiquitin ligase (Bhaumik and Malik 2008). In yeast, Rad6 and Bre1 are the E2 ubiquitin conjugase and E3 ubiquitin ligase for histone H2B monoubiquitylation, respectively (Xiao *et al.* 2005; Bhaumik *et al.* 2007; Shukla and Bhaumik 2007; Tanny *et al.* 2007; Fleming *et al.* 2008; Shukla *et al.* 2009; Sen and Bhaumik 2013; Sen *et al.* 2013). Such histone H2B ubiquitylation facilitates transcription elongation (Xiao *et al.* 2005; Shukla and Bhaumik 2007; Tanny *et al.* 2007; Fleming *et al.* 2008; Sen *et al.* 2013). Histone H2B ubiquitylation is reversed by ubiquitin protease (or DUB), Ubp8, present within the DUB module of SAGA (Köhler *et al.* 2010; Samara *et al.* 2010; Bhaumik 2011; Samara *et al.* 2012; Cheon *et al.* 2020). Thus, histone H2B ubiquitylation is increased in the *Δubp8* strain (Henry *et al.* 2003; Shukla, Stanojevic, *et al.* 2006). Intriguingly, increased level of histone H2B ubiquitylation in the absence of Ubp8 impairs transcription elongation (Wyce *et al.* 2007), even though histone H2B ubiquitylation is known to facilitate transcription elongation (Xiao *et al.* 2005; Shukla and Bhaumik 2007; Tanny *et al.* 2007; Fleming *et al.* 2008; Sen *et al.* 2013). Thus, histone H2B ubiquitylation is fine-tuned by E3 ubiquitin ligase, Bre1, and DUB, Ubp8, for optimal transcription elongation. Alteration of this balancing act impairs transcription elongation (Shukla and Bhaumik 2007; Wyce *et al.* 2007; Sen and Bhaumik 2013; Sen *et al.* 2013). Thus, increased or decreased deubiquitylation of ubiquitylated histone H2B would alter the level of histone H2B ubiquitylation to reduce transcription elongation. Histone H2B deubiquitylation can be decreased via the downregulation of the DUB activity of Ubp8. Sgf73 is required for the DUB activity of Ubp8 (Lee, Florens, *et al.* 2005; Köhler *et al.* 2008; Köhler *et al.* 2010) and, thus, decreased abundance of Sgf73 would lower Ubp8's DUB activity, leading to increased histone H2B ubiquitylation (Köhler *et al.* 2008). Indeed, increased histone H2B ubiquitylation was observed in the absence of Sgf73 (Kohler *et al.* 2008; Lee *et al.* 2009). Such increased level of histone H2B ubiquitylation would reduce transcription elongation, as increased histone H2B ubiquitylation in the absence of Ubp8 has shown reduced transcription elongation (Wyce *et al.* 2007). In agreement, we also observed cellular growth defect in 6-AU (Supplementary Fig. 4a), when the cellular abundance of Sgf73 was reduced (Fig. 8a and b), leading to decreased DUB activity of Ubp8 (Lee, Florens, *et al.* 2005; Kohler *et al.* 2008, 2010) and increased histone H2B ubiquitylation. Consistently, the *Δsgf73* strain also shows the growth defect in 50 μg/ml 6-AU as well as reduced association of RNA polymerase II and Sus1 with the active gene (Pascual-García *et al.* 2008). Unlike the growth defect phenotype of the *Δsgf73* strain in 6-AU (Pascual-García *et al.* 2008), *Δsgf73* is not sensitive to MPA (Malik *et al.* 2017). Likewise, we do not observe the growth defect in MPA, when cellular Sgf73 level was reduced (Supplementary Fig. 4b). MPA depletes *g*uanosine *t*ri*p*hosphate (GTP) by inhibiting the inosine *m*onophosphate *d*e*h*ydrogenase (IMPDH) activities encoded by 2 MPA-sensitive IMPDH paralogs, namely *IMD3* and *IMD4*. Decreased level of GTP in the presence of MPA induces the expression of *IMD2* via switching of the transcription start site, which contributes to the MPA resistance (Malik *et al.* 2017). Like MPA, 6-AU is also involved in inhibiting IMPDH (as well as orotidylate decarboxylase) to limit nucleotide pool for transcription elongation (Riles *et al.* 2004). However, the mechanism of action of 6-AU is less understood in comparison with well-known mechanism of uncompetitive inhibition of IMPDH by MPA (Riles *et al.* 2004). Since 6-AU and MPA have different inhibition activities, not all mutants are equally sensitive to 6-AU and MPA (Riles *et al.* 2004), as was observed for *Δsgf73* (Pascual-García *et al.* 2008) or in the absence of Sgf73 (Supplementary Fig. 4). Yet, there is a large of overlap of the mutants showing growth sensitivities to both 6-AU and MPA (Riles *et al.* 2004).

We find that increased abundance of Sgf73 reduced transcription elongation (Figs. 4–6). As mentioned above, Sgf73 is required for SAGA's integrity and the DUB activity of Ubp8 (Lee, Florens, *et al.* 2005; Köhler et al. 2006; Shukla, Bajwa, and Bhaumik 2006; Köhler et al. 2008; Lee *et al.* 2009; Köhler *et al.* 2010; Durand *et al.* 2014; Morgan *et al.* 2016; Wang *et al.* 2020). Thus, increased abundance of Sgf73 could enhance Ubp8's DUB activity, leading to decreased histone H2B ubiquitylation and consequently reduced transcription elongation (as decreased level of histone H2B ubiquitylation impairs transcription elongation; Shukla and Bhaumik 2007; Sen and Bhaumik 2013; Sen *et al.* 2013). Alternatively, SAGA–associated Sgf73 interacts with the DUB components to assemble whole SAGA during transcription, and increased abundance of free Sgf73 could compete with SAGA–associated Sgf73 to form DUB module outside SAGA, leading to impairment of DUB-containing whole SAGA assembly and hence altered transcription elongation. According to this model, one would expect to observe less recruitment of the DUB component, but not Sgf73 or core SAGA component (e.g. Spt20), to the UAS of the SAGA–regulated gene in response to increased abundance of Sgf73, and existence of DUB module without SAGA. Indeed, we observed decreased recruitment of the key DUB module component, Ubp8, but not core SAGA component (Spt20) or Sgf73, to the SAGA–regulated *GAL1* UAS in response to increase abundance of Sgf73 (Fig. 7), and the DUB module is found to exist without SAGA (Köhler *et al.* 2008). Thus, our results indicate DUB-depleted SAGA in the presence of high abundance of Sgf73, which would alter histone H2B ubiquitylation, leading to the defect in transcription elongation (as both increased and decreased levels of histone H2B ubiquitylation impair transcription elongation; Xiao *et al.* 2005; Shukla and Bhaumik 2007; Wyce *et al.* 2007; Fleming *et al.* 2008; Sen and Bhaumik 2013; Sen *et al.* 2013; Durairaj, Sen, *et al.* 2014). Indeed, we observe the defect in transcription elongation in the presence of high abundance of Sgf73

Fig. 10. (Continued)
analyzed in cBioPortal. The frequencies of 0.1% and above were plotted with a minimum sample number of 3. f) Ataxin-7 levels were analyzed in kidney, lung, and uterine cancer patients based on Clinical Proteomic Tumor Analysis Consortium (CPTAC) samples using the UALCAN web portal. The Z values for ataxin-7 in normal and cancer samples are plotted. KIRC, *k*idney renal clear cell *c*arcinoma; LUAD, *l*ung *ad*enocarcinoma; and UCEC, *u*terine *c*orpus *e*ndometrial *c*arcinoma. g) *ATXN7* mRNA levels in kidney, lung, and uterine cancer patients based on The Cancer Genome Atlas (TCGA) samples using the UALCAN web portal.

(Figs. 4–6). Further, it is possible that DUB module might be interfering the interaction of SAGA with TBP, as DUB and TBP–interacting modules of SAGA are located closely to each other (Wang et al. 2020). In fact, we observe increased TBP association with the promoter in the presence of high abundance of Sgf73 (Fig. 3c–e) that reduces recruitment of DUB module, but not core SAGA, to the gene (Fig. 7). Further, it may be possible that impairment of transcription elongation in the presence of high abundance of Sgf73 might be slowing down the PIC disassembly (or transitioning of transcription initiating RNA polymerase II to elongation), thereby enhancing the PIC's residence time at the promoter (and hence formaldehyde-based cross-linking and consequently increased ChIP signal). Nonetheless, our results reveal the defect in transcription elongation in the presence of high abundance of Sgf73 (Figs. 4–6), consistent with decreased gene association of Ubp8 (Fig. 7b), and such defect in transcription elongation might be indirectly enhancing the association of TBP with promoter. In addition or alternatively, DUB-depleted SAGA in the presence of high abundance of Sgf73 might be more efficient to recruit TBP to the promoter in comparison with the whole SAGA, which remains to be further elucidated.

Our results show that alteration of Sgf73 abundance/stability affects the association of TBP and RNA polymerase II with the active genes and hence transcription. Thus, Sgf73 abundance needs to be fine-tuned for its optimal function. Our results reveal the fine-tuning of Sgf73 by UPS (Figs. 1 and 2). Consistent with our results, previous global analysis also indicated ubiquitylation of Sgf73 (Swaney et al. 2013), but its regulation by the 26S proteasome was unknown. Our results reveal the ubiquitylation and proteasomal degradation of Sgf73. Further, the K48 (lysine 48)-linked polyubiquitin chain undergoes 26S proteasomal degradation (Bhaumik and Malik 2008), and thus, Sgf73 is likely to be polyubiquitylated through K48 linkage for proteasomal degradation. Moreover, since Sgf73 and UPS are conserved in humans, Sgf73's human homologue, ataxin-7, is likely to be regulated by ubiquitylation and proteasomal degradation. Indeed, we find that ataxin-7 undergoes ubiquitylation and proteasomal degradation (Fig. 10a–d). Increased or decreased level of ataxin-7 in response to alteration of such UPS regulation would affect transcription. Indeed, increased or decreased level of ataxin-7 is found to alter transcription in human cells (Palhan et al. 2005; Ström et al. 2005; Guha et al. 2022), similar to the results in yeast. Further, ataxin-7 is found to complement the function of Sgf73 in yeast (McMahon et al. 2005). Thus, our results reveal a conserved UPS regulation of Sgf73/ataxin-7 in yeast as well as humans with physiological relevance. Further, ataxin-7 is found to be up and downregulated in various cancer patient samples (Fig. 10e–g) and other diseases such as childhood blindness, neurodegenerative disorder, attention deficit/hyperactivity disorder, and ocular coloboma (Holmberg et al. 1998; Lindenberg et al. 2000; Yvert et al. 2001; Yoo et al. 2003; Michalik et al. 2004; Palhan et al. 2005; Helmlinger, Hardy, et al. 2006; Helmlinger, Tora, and Devys 2006; Garden and La Spada 2008; Rüb et al. 2008; McCullough et al. 2012; Yanicostas et al. 2012; Mohan, Abmayr, and Workman 2014; Mohan, Dialynas, et al. 2014; Karam and Trottier 2018; Carrillo-Rosas et al. 2019; Dela Peña et al. 2019; Niewiadomska-Cimicka and Trottier 2019; Cornelio-Parra et al. 2021). Thus, our results implicate the alteration of UPS regulation of ataxin-7 in these diseases. In agreement, ataxin-7 protein level, but not mRNA, is found to be increased in different cancer patient samples (Fig. 10f and g).

In summary, our results demonstrate that increased or decreased abundance of Sgf73 is linked to altered association of TBP and RNA polymerase II with genes and hence transcription in yeast. Thus, Sgf73 needs to be fine-tuned for optimal transcription. We show here that UPS maintains the cellular level of Sgf73 in yeast. Like in yeast, human ataxin-7 undergoes ubiquitylation and proteasomal degradation. Alteration of such regulation is likely to be associated with cancer, neurodegenerative disorder, attention deficit/hyperactivity disorder, ocular coloboma, childhood blindness, and other diseases (as ataxin-7 is found to be upregulated or downregulated in various cancer patient samples and disease states), which remains to be further elucidated toward searching for new etiologies of these diseases. Nevertheless, our results unveil here a novel UPS regulation for Sgf73/ataxin-7 in maintaining normal cellular health and open a new avenue for future research with implications in disease pathogenesis and therapeutic interventions.

Data availability

Strains are available upon request. All data necessary for confirming the conclusions are present within the article, figures, and Supplementary Material.

Supplemental material available at GENETICS online.

Acknowledgments

We thank Judith K. Davie for the tissue culture facility; Michael R. Green for TBP antibody; Kevin Struhl, Thomas Kodadek, and Stephen Johnston for yeast strains; Daniel Finley and Manas K. Santra for plasmids; and Divya Reddy for technical assistance.

Funding

The work in the Bhaumik laboratory was supported by the grants from National Institutes of Health (2R15GM088798-02 and 2R15GM088798-03), American Heart Association (15GRNT25700298), and Southern Illinois University School of Medicine and Cancer Institute.

Conflicts of interest

The author(s) declare no conflict of interest.

Literature cited

Baker SP, Grant PA. The SAGA continues: expanding the cellular role of a transcriptional co-activator complex. Oncogene 2007;26(37):5329–5340. doi:10.1038/sj.onc.1210603.

Bhaumik SR. Distinct regulatory mechanisms of eukaryotic transcriptional activation mediated by SAGA and TFIID. Biochim Biophys Acta. 2011;1809(2):97–108. doi:10.1016/j.bbagrm.2010.08.009.

Bhaumik SR, Green MR. SAGA Is an essential in vivo target of the yeast acidic activator Gal4p. Genes Dev. 2001;15(15):1935–1945. doi:10.1101/gad.911401.

Bhaumik SR, Green MR. Differential requirement of SAGA components for recruitment of TATA-box-binding protein to promoters in vivo. Mol Cell Biol. 2002;22(21):7365–7371. doi:10.1128/MCB.22.21.7365-7371.2002.

Bhaumik SR, Green MR. Interaction of Gal4p with components of transcription machinery in vivo. Methods Enzymol. 2003;370:445–454. doi:10.1016/S0076-6879(03)70038-X.

Bhaumik SR, Malik S. Diverse regulatory mechanisms of eukaryotic transcriptional activation by the proteasome complex. Crit Rev

Biochem Mol Biol. 2008;43(6):419–433. doi:10.1080/10409230802605914.

Bhaumik SR, Raha T, Aiello DP, Green MR. In vivo target of a transcriptional activator revealed by fluorescence resonance energy transfer. Genes Dev. 2004;18(3):333–343. doi:10.1101/gad.1148404.

Bhaumik SR, Smith E, Shilatifard A. Covalent modifications of histones during development and disease pathogenesis. Nat Struct Mol Biol. 2007;14(11):1008–1016. doi:10.1038/nsmb1337.

Bonnet J, Wang C-Y, Baptista T, Vincent SD, Hsiao W-C, Stierle M, Kao C-F, Tora L, Devys D. The SAGA coactivator complex acts on the whole transcribed genome and is required for RNA polymerase II transcription. Genes Dev. 2014;28(18):1999–2012. doi:10.1101/gad.250225.114.

Brown CE, Howe L, Sousa K, Alley SC, Carrozza MJ, Tan S, and Workman JL. Recruitment of HAT complexes by direct activator interactions with the ATM-related Tra1 subunit. Science 2001;292(5525):2333–2337. doi:10.1126/science.1060214.

Carrillo-Rosas S, Weber C, Fievet L, Messaddeq N, Karam A, Trottier Y. Loss of zebrafish ataxin-7, a SAGA subunit responsible for SCA7 retinopathy, causes ocular coloboma and malformation of photoreceptors. Hum Mol Genet. 2019;28(6):912–927. doi:10.1093/hmg/ddy401.

Cerami E, Gao J, Dogrusoz U, Gross BE, Sumer SO, Aksoy BA, Jacobsen A, Byrne CJ, Heuer ML, Larsson E, *et al.* The cBio cancer genomics portal: an open platform for exploring multidimensional cancer genomics data. Cancer Discov. 2012;2(5):401–404. doi:10.1158/2159-8290.CD-12-0095.

Chandrashekar DS, Bashel B, Balasubramanya SAH, Creighton CJ, Ponce-Rodriguez I, Chakravarthi BVSK, Varambally S. UALCAN: a portal for facilitating tumor subgroup gene expression and survival analyses. Neoplasia 2017;19(8):649–658. doi:10.1016/j.neo.2017.05.002.

Chen F, Chandrashekar DS, Varambally S, Creighton CJ. Pan-cancer molecular subtypes revealed by mass-spectrometry-based proteomic characterization of more than 500 human cancers. Nat Commun. 2019;10(1):5679. doi:10.1038/s41467-019-13528-0.

Chen YC, Dent SYR. Conservation and diversity of the eukaryotic SAGA coactivator complex across kingdoms. Epigenetics Chromatin 2021;14(1):26. doi:10.1186/s13072-021-00402-x.

Cheon Y, Kim H, Park K, Kim M, Lee D. Dynamic modules of the coactivator SAGA in eukaryotic transcription. Exp Mol Med. 2020;52(7):991–1003. doi:10.1038/s12276-020-0463-4.

Cornelio-Parra DV, Goswami R, Costanzo K, Morales-Sosa P, Mohan RD. Function and regulation of the Spt-Ada-Gcn5-Acetyltransferase (SAGA) deubiquitinase module. Biochim Biophys Acta Gene Regul Mech. 2021;1864(2):194630. doi:10.1016/j.bbagrm.2020.194630.

Davis CF, Ricketts CJ, Wang M, Yang L, Cherniack AD, Shen H, Buhay C, Kang H, Kim SC, Fahey CC, *et al.* The somatic genomic landscape of chromophobe renal cell carcinoma. Cancer Cell 2014;26(3):319–330. doi:10.1016/j.ccr.2014.07.014.

Dela Peña IJI, Botanas CJ, de la Peña JB, Custodio RJ, Dela Peña I, Ryoo ZY, Kim BN, Ryu JH, Kim HJ, Cheong JH. The Atxn7-overexpressing mice showed hyperactivity and impulsivity which were ameliorated by atomoxetine treatment: a possible animal model of the hyperactive-impulsive phenotype of ADHD. Prog Neuropsychopharmacol Biol Psychiatry. 2019;88:311–319. doi:10.1016/j.pnpbp.2018.08.012.

Dudley AM, Rougeulle C, and Winston F. The Spt components of SAGA facilitate TBP binding to a promoter at a post-activator-binding step in vivo. Genes Dev. 1999;13(22):2940–2945. doi:10.1101/gad.13.22.2940.

Durairaj G, Lahudkar S, Bhaumik SR. A new regulatory pathway of mRNA export by an F-box protein, Mdm30. RNA 2014;20(2):133–142. doi:10.1261/rna.042325.113.

Durairaj G, Malik S, Bhaumik SR. Regulatory mechanisms of eukaryotic gene expression. In: Mandal S, editor. Gene Regulation, Epigenetics and Hormone Signaling. Germany: Wiley-VCH; 2017. Volume 1, p. 1–28 .

Durairaj G, Sen R, Uprety B, Shukla A, Bhaumik SR. Sus1p facilitates pre-initiation complex formation at the SAGA-regulated genes independently of histone H2B de-ubiquitylation. J Mol Biol. 2014;426(16):2928–2941. doi:10.1016/j.jmb.2014.05.028.

Durand A, Bonnet J, Fournier M, Chavant V, Schultz P. Mapping the deubiquitination module within the SAGA complex. Structure 2014;22(11):1553–1559. doi:10.1016/j.str.2014.07.017.

Espinola-Lopez JM, Tan S. The Ada2/Ada3/Gcn5/Sgf29 histone acetyltransferase module. Biochim Biophys Acta Gene Regul Mech. 2021;1864(2):194629. doi:10.1016/j.bbagrm.2020.194629.

Ferdoush J, Karmakar S, Barman P, Kaja A, Uprety B, Batra SK, Bhaumik SR. Ubiquitin-proteasome system regulation of an evolutionarily conserved RNA polymerase II-associated factor 1 involved in pancreatic oncogenesis. Biochemistry 2017;56(46):6083–6086. doi:10.1021/acs.biochem.7b00865.

Fleming AB, Kao CF, Hillyer C, Pikaart M, Osley MA. H2b ubiquitylation plays a role in nucleosome dynamics during transcription elongation. Mol Cell. 2008;31(1):57–66. doi:10.1016/j.molcel.2008.04.025.

Furrer SA, Mohanachandran MS, Waldherr SM, Chang C, Damian VA, Sopher BL, Garden GA, La Spada AR. SCA7 cerebellar disease requires the coordinated action of mutant ataxin-7 in neurons and glia, and displays non-cell autonomous Bergmann glia degeneration. J Neurosci. 2011;31(45):16269–16278. doi:10.1523/JNEUROSCI.4000-11.2011.

Gao J, Aksoy BA, Dogrusoz U, Dresdner G, Gross B, Sumer SO, Sun Y, Jacobsen A, Sinha R, Larsson E, *et al.* Integrative analysis of complex cancer genomics and clinical profiles using the cBioPortal. Sci Signal. 2013;6(269):l1. doi:10.1126/scisignal.2004088.

Garden GA, La Spada AR. Molecular pathogenesis and cellular pathology of spinocerebellar ataxia type 7 neurodegeneration. Cerebellum 2008;7(2):138–149. doi:10.1007/s12311-008-0027-y.

Grant PA, Winston F, Berger SL. The biochemical and genetic discovery of the SAGA complex. Biochim Biophys Acta Gene Regul Mech. 2021;1864(2):194669. doi:10.1016/j.bbagrm.2020.194669.

Guha S, Barman P, Manawa A, Bhaumik SR. Nuclear export of mRNAs with disease pathogenesis and therapeutic implications. In: Jurga S, Barciszewski J, editors. Messenger RNA therapeutics. Switzerland: Springer Nature; 2022. p. 371-395.

Helmlinger D, Hardy S, Abou-Sleymane G, Eberlin A, Bowman AB, Gansmüller A, Picaud S, Zoghbi HY, Trottier Y, Tora L, *et al.* Glutamine-expanded ataxin-7 alters TFTC/STAGA recruitment and chromatin structure leading to photoreceptor dysfunction. PLoS Biol. 2006;4(3):e67. doi:10.1371/journal.pbio.0040067.

Helmlinger D, Tora L, Devys D. Transcriptional alterations and chromatin remodeling in polyglutamine diseases. Trends Genet. 2006;22(10):562–570. doi:10.1016/j.tig.2006.07.010.

Henry KW, Wyce A, Lo WS, Duggan LJ, Emre NC, Kao CF, Pillus L, Shilatifard A, Osley MA, Berger SL. Transcriptional activation via sequential histone H2B ubiquitylation and deubiquitylation, mediated by SAGA-associated Ubp8. Genes Dev. 2003;17(21):2648–2663. doi:10.1101/gad.1144003.

Holmberg M, Duyckaerts C, Dürr A, Cancel G, Gourfinkel-An I, Damier P, Faucheux B, Trottier Y, Hirsch EC, Agid Y, *et al.* Spinocerebellar ataxia type 7 (SCA7): a neurodegenerative disorder with neuronal intranuclear inclusions. Hum Mol Genet. 1998;7(5):913–918. doi:10.1093/hmg/7.5.913.

Holstege FC, Jennings EG, Wyrick JJ, Lee TI, Hengartner CJ, Green MR, Golub TR, Lander ES, Young RA. Dissecting the regulatory

circuitry of a eukaryotic genome. Cell 1998;95(5):717–728. doi:10.1016/S0092-8674(00)81641-4.

Huisinga KL, Pugh BF. A genome-wide housekeeping role for TFIID and a highly regulated stress-related role for SAGA in *Saccharomyces cerevisiae*. Mol Cell. 2004;13(4):573–585. doi:10.1016/S1097-2765(04)00087-5.

Kaja A, Adhikari A, Karmakar S, Zhang W, Rothschild G, Basu U, Batra SK, Davie JK, Bhaumik SR. Proteasomal regulation of mammalian SPT16 in controlling transcription. Mol Cell Biol. 2021;41(4):e00452-20. doi:10.1128/MCB.00452-20.

Kapoor S. Usp22 and its evolving role in systemic carcinogenesis. Lung Cancer 2013;79(2):191. doi:10.1016/j.lungcan.2012.11.002.

Karam A, Trottier Y. Molecular mechanisms and therapeutic strategies in spinocerebellar ataxia type 7. Adv Exp Med Biol. 2018;1049:197–218. doi:10.1007/978-3-319-71779-1_9.

Karmakar S, Ponnusamy MP, Bhaumik SR, Batra SK. RNA polymerase II and Associated Transcription Factors. Encyclopedia in Life Science (eLS). Chichester: John Wiley & Sons, Ltd; 2018.

Köhler A, Pascual-García P, Llopis A, Zapater M, Posas F, Hurt E, Rodríguez-Navarro S. The mRNA export factor Sus1 is involved in Spt/Ada/Gcn5 acetyltransferase-mediated H2B deubiquitinylation through its interaction with Ubp8 and Sgf11. Mol Biol Cell. 2006;17(10):4228–4236. doi:10.1091/mbc.e06-02-0098.

Köhler A, Schneider M, Cabal GG, Nehrbass U, Hurt E. Yeast Ataxin-7 links histone deubiquitination with gene gating and mRNA export. Nat Cell Biol. 2008;10(6):707–715. doi:10.1038/ncb1733.

Köhler A, Zimmerman E, Schneider M, Hurt E, Zheng N. Structural basis for assembly and activation of the heterotetrameric SAGA histone H2B deubiquitinase module. Cell 2010;141(4):606–617. doi:10.1016/j.cell.2010.04.026.

Lang G, Bonnet J, Umlauf D, Karmodiya K, Koffler J, Stierle M, Devys D, Tora L. The tightly controlled deubiquitination activity of the human SAGA complex differentially modifies distinct gene regulatory elements. Mol Cell Biol. 2011;31(18):3734–3744. doi:10.1128/MCB.05231-11.

Larschan E, Winston F. The *S. cerevisiae* SAGA complex functions in vivo as a coactivator for transcriptional activation by Gal4. Genes Dev. 2001;15(15):1946–1956. doi:10.1101/gad.911501.

Lee D, Ezhkova E, Li B, Pattenden SG, Tansey WP, Workman JL. The proteasome regulatory particle alters the SAGA coactivator to enhance its interactions with transcriptional activators. Cell 2005;123(3):423–436. doi:10.1016/j.cell.2005.08.015.

Lee KK, Florens L, Swanson SK, Washburn MP, Workman JL. The deubiquitylation activity of Ubp8 is dependent upon Sgf11 and its association with the SAGA complex. Mol Cell Biol. 2005;25(3):1173–1182. doi:10.1128/MCB.25.3.1173-1182.2005.

Lee KK, Sardiu ME, Swanson SK, Gilmore JM, Torok M, Grant PA, Florens L, Workman JL, Washburn MP. Combinatorial depletion analysis to assemble the network architecture of the SAGA and ADA chromatin remodeling complexes. Mol Syst Biol. 2011;7(1):503. doi:10.1038/msb.2011.40.

Lee KK, Swanson SK, Florens L, Washburn MP, Workman JL. Yeast Sgf73/Ataxin-7 serves to anchor the deubiquitination module into both SAGA and Slik(SALSA) HAT complexes. Epigenetics Chromatin 2009;2(1):2. doi:10.1186/1756-8935-2-2.

Li X-Y, Bhaumik SR, Green MR. Distinct classes of yeast promoters revealed by differential TAF recruitment. Science 2000;288(5469):1242–1244. doi:10.1126/science.288.5469.1242.

Li C, Irrazabal T, So CC, Berru M, Du L, Lam E, Ling AK, Gommerman JL, Pan-Hammarstrom Q, Martin A. The H2B deubiquitinase Usp22 promotes antibody class switch recombination by facilitating non-homologous end joining. Nat Commun. 2018;9(1):1006. doi:10.1038/s41467-018-03455-x.

Lim S, Kwak J, Kim M, Lee D. Separation of a functional deubiquitylating module from the SAGA complex by the proteasome regulatory particle. Nat Commun. 2013;4(1):2641. doi:10.1038/ncomms3641.

Lindenberg KS, Yvert G, Müller K, Landwehrmeyer GB. Expression analysis of ataxin-7 mRNA and protein in human brain: evidence for a widespread distribution and focal protein accumulation. Brain Pathol. 2000;10(3):385–394. doi:10.1111/j.1750-3639.2000.tb00270.x.

Lipford JR, Smith GT, Chi Y, Deshaies RJ. A putative stimulatory role for activator turnover in gene expression. Nature 2005;438(7064):113–116. doi:10.1038/nature04098.

Longtine MS, McKenzie A 3rd, Demarini DJ, Shah NG, Wach A, Brachat A, Philippsen P, Pringle JR. Additional modules for versatile and economical PCR-based gene deletion and modification in *Saccharomyces cerevisiae*. Yeast 1998;14(10):953–961. doi:10.1002/(SICI)1097-0061(199807)14:10<953::AID-YEA293>3.0.CO;2-U.

Malik I, Qiu C, Snavely T, Kaplan CD. Wide-ranging and unexpected consequences of altered Pol II catalytic activity in vivo. Nucleic Acids Res. 2017;45(8):4431–4451. doi:10.1093/nar/gkx037.

Malik S, Shukla A, Sen P, Bhaumik SR. The 19S proteasome subcomplex establishes a specific protein interaction network at the promoter for stimulated transcriptional initiation in vivo. J Biol Chem. 2009;284(51):35714–35724. doi:10.1074/jbc.M109.035709.

Malonia SK, Dutta P, Santra MK, Green MR. F-box protein FBXO31 directs degradation of MDM2 to facilitate p53-mediated growth arrest following genotoxic stress. Proc Natl Acad Sci U S A. 2015;112(28):8632–8637. doi:10.1073/pnas.1510929112.

Mason PB, Struhl K. Distinction and relationship between elongation rate and processivity of RNA polymerase II in vivo. Mol Cell. 2005;17(6):831–840. doi:10.1016/j.molcel.2005.02.017.

McCullough SD, Xu X, Dent SYR, Bekiranov S, Roeder RG, Grant PA. Reelin is a target of polyglutamine expanded ataxin-7 in human spinocerebellar ataxia type 7 (SCA7) astrocytes. Proc Natl Acad Sci U S A. 2012;109(52):21319–21324. doi:10.1073/pnas.1218331110.

McMahon SJ, Pray-Grant MG, Schieltz D, Yates JR 3rd, Grant PA. Polyglutamine-expanded spinocerebellar ataxia-7 protein disrupts normal SAGA and SLIK histone acetyltransferase activity. Proc Natl Acad Sci U S A. 2005;102(24):8478–8482. doi:10.1073/pnas.0503493102.

Melo-Cardenas J, Xu Y, Wei J, Tan C, Kong S, Gao B, Montauti E, Kirsammer G, Licht JD, Yu J, *et al.* USP22 Deficiency leads to myeloid leukemia upon oncogenic Kras activation through a PU.1-dependent mechanism. Blood 2018;132(4):423–434. doi:10.1182/blood-2017-10-811760.

Michalik A, Martin JJ, Van Broeckhoven C. Spinocerebellar ataxia type 7 associated with pigmentary retinal dystrophy. Eur J Hum Genet. 2004;12(1):2–15. doi:10.1038/sj.ejhg.5201108.

Mohan RD, Abmayr SM, Workman JL. Pulling complexes out of complex diseases: spinocerebellar ataxia 7. Rare Dis. 2014;2(1):e28859. doi:10.4161/rdis.28859.

Mohan RD, Dialynas G, Weake VM, Liu J, Martin-Brown S, Florens L, Washburn MP, Workman JL, Abmayr SM. Loss of Drosophila ataxin-7, a SAGA subunit, reduces H2B ubiquitination and leads to neural and retinal degeneration. Genes Dev. 2014;28(3):259–272. doi:10.1101/gad.225151.113.

Morgan MT, Haj-Yahya M, Ringel AE, Bandi P, Brik A, Wolberger C. Structural basis for histone H2B deubiquitination by the SAGA DUB module. Science 2016;351(6274):725–728. doi:10.1126/science.aac5681.

Niewiadomska-Cimicka A, Trottier Y. Molecular targets and therapeutic strategies in spinocerebellar ataxia type 7. Neurotherapeutics 2019;16(4):1074–1096. doi:10.1007/s13311-019-00778-5.

Palhan VB, Chen S, Peng G-H, Tjernberg A, Gamper AM, Fan Y, Chait BT, La Spada AR, Roeder RG. Polyglutamine-expanded ataxin-7 inhibits STAGA histone acetyltransferase activity to produce retinal degeneration. Proc Natl Acad Sci U S A. 2005;102(24):8472–8477. doi:10.1073/pnas.0503505102.

Pascual-García P, Govind CK, Queralt E, Cuenca-Bono B, Llopis A, Chavez S, Hinnebusch AG, Rodríguez-Navarro S. Sus1 is recruited to coding regions and functions during transcription elongation in association with SAGA and TREX2. Genes Dev. 2008;22(20):2811–2822. doi:10.1101/gad.483308.

Riles L, Shaw RJ, Johnston M, Reines D. Large-scale screening of yeast mutants for sensitivity to the IMP dehydrogenase inhibitor 6-azauracil. Yeast 2004;21(3):241–248. doi:10.1002/yea.1068.

Ristic G, Tsou WL, Todi SV. An optimal ubiquitin-proteasome pathway in the nervous system: the role of deubiquitinating enzymes. Front Mol Neurosci. 2014;7:72. doi:10.3389/fnmol.2014.00072.

Rodriguez-Navarro S. Insights into SAGA function during gene expression. EMBO Rep. 2009;10(8):843–850. doi:10.1038/embor.2009.168.

Rüb U, Brunt ER, Seidel K, Gierga K, Mooy CM, Kettner M, Van Broeckhoven C, Bechmann I, La Spada AR, Schöls L, *et al.* Spinocerebellar ataxia type 7 (SCA7): widespread brain damage in an adult-onset patient with progressive visual impairments in comparison with an adult-onset patient without visual impairments. Neuropathol Appl Neurobiol. 2008;34(2):155–168. doi:10.1111/j.1365-2990.2007.00882.x.

Rubin DM, Glickman MH, Larsen CN, Dhruvakumar S, Finley D. Active site mutants in the six regulatory particle ATPases reveal multiple roles for ATP in the proteasome. EMBO J. 1998;17(17):4909–4919. doi:10.1093/emboj/17.17.4909.

Russell SJ, Gonzalez F, Joshua-Tor L, Johnston SA. Selective chemical inactivation of AAA proteins reveals distinct functions of proteasomal ATPases. Chem Biol. 2001;8(10):941–950. doi:10.1016/S1074-5521(01)00060-6.

Russell SJ, Johnston SA. Evidence that proteolysis of Gal4 cannot explain the transcriptional effects of proteasome ATPase mutations. J Biol Chem. 2001;276(13):9825–9831. doi:10.1074/jbc.M010889200.

Samara NL, Datta AB, Berndsen CE, Zhang X, Yao T, Cohen RE, Wolberger C. Structural insights into the assembly and function of the SAGA deubiquitinating module. Science 2010;328(5981):1025–1029. doi:10.1126/science.1190049.

Samara NL, Ringel AE, Wolberger C. A role for intersubunit interactions in maintaining SAGA deubiquitinating module structure and activity. Structure 2012;20(8):1414–1424. doi:10.1016/j.str.2012.05.015.

Schrecengost RS, Dean JL, Goodwin JF, Schiewer MJ, Urban MW, Stanek TJ, Sussman RT, Hicks JL, Birbe RC, Draganova-Tacheva RA, *et al.* USP22 regulates oncogenic signaling pathways to drive lethal cancer progression. Cancer Res. 2014;74(1):272–286. doi:10.1158/0008-5472.CAN-13-1954.

Sen R, Bhaumik SR. Transcriptional stimulatory and repressive functions of histone H2B ubiquitin ligase. Transcription 2013;4(5):221–226. doi:10.4161/trns.26623.

Sen R, Ferdoush J, Kaja A, Bhaumik SR. Fine-tuning of FACT by ubiquitin proteasome system in regulation of transcriptional elongation. Mol Cell Biol. 2016;36(11):1691–1703. doi:10.1128/MCB.01112-15.

Sen R, Lahudkar S, Durairaj G, Bhaumik SR. Functional analysis of Bre1p, an E3 ligase for histone H2B ubiquitylation, in regulation of RNA polymerase II association with active genes and transcription in vivo. J Biol Chem. 2013;288(14):9619–9633. doi:10.1074/jbc.M113.450403.

Sermwittayawong D, Tan S. SAGA Binds TBP via its Spt8 subunit in competition with DNA: implications for TBP recruitment. EMBO J. 2006;25(16):3791–3800. doi:10.1038/sj.emboj.7601265.

Shukla A, Bajwa P, Bhaumik SR. SAGA-associated Sgf73p facilitates formation of the preinitiation complex assembly at the promoters either in a HAT-dependent or independent manner in vivo. Nucleic Acids Res. 2006;34(21):6225–6232. doi:10.1093/nar/gkl844.

Shukla A, Bhaumik SR. H2B-K123 ubiquitination stimulates RNAPII elongation independent of H3-K4 methylation. Biochem Biophys Res Commun. 2007;359(2):214–220. doi:10.1016/j.bbrc.2007.05.105.

Shukla A, Chaurasia P, Bhaumik SR. Histone methylation and ubiquitination with their cross-talk and roles in gene expression and stability. Cell Mol Life Sci. 2009;66(8):1419–1433. doi:10.1007/s00018-008-8605-1.

Shukla A, Lahudkar S, Durairaj G, Bhaumik SR. Sgf29p facilitates the recruitment of TATA-box-binding protein, but does not alter SAGA's global structural integrity *in vivo*. Biochemistry 2012;51(2):706–714. doi:10.1021/bi201708z.

Shukla A, Stanojevic N, Duan Z, Sen P, Bhaumik SR. Ubp8p, a histone deubiquitinase whose association with SAGA is mediated by Sgf11p, differentially regulates lysine 4 methylation of histone H3 in vivo. Mol Cell Biol. 2006;26(9):3339–3352. doi:10.1128/MCB.26.9.3339-3352.2006.

Sikorski RS, Hieter P. A system of shuttle vectors and yeast host strains designed for efficient manipulation of DNA in *Saccharomyces cerevisiae*. Genetics 1989;122(1):19–27. doi:10.1093/genetics/122.1.19.

Soffers JHM, Workman JL. The SAGA chromatin-modifying complex: the sum of its parts is greater than the whole. Genes Dev. 2020;34(19–20):1287–1303. doi:10.1101/gad.341156.120.

Spedale G, Timmers HT, Pijnappel WW. ATAC-king the complexity of SAGA during evolution. Genes Dev. 2012;26(6):527–541. doi:10.1101/gad.184705.111.

Sterner DE, Grant PA, Roberts SM, Duggan LJ, Belotserkovkaya R, Pacella LA, Winston F, Workman JL, Berger SL. Functional organization of the yeast SAGA complex: distinct components involved in structural integrity, nucleosome acetylation, and TATA-binding protein interaction. Mol Cell Biol. 1999;19(1):86–98. doi:10.1128/MCB.19.1.86.

Ström AL, Forsgren L, Holmberg M. A role for both wild-type and expanded ataxin-7 in transcriptional regulation. Neurobiol Dis. 2005;20(3):646–655. doi:10.1016/j.nbd.2005.04.018.

Swaney DL, Beltrao P, Starita L, Guo A, Rush J, Fields S, Krogan NJ, Villén J. Global analysis of phosphorylation and ubiquitylation cross-talk in protein degradation. Nat Methods. 2013;10(7):676–682. doi:10.1038/nmeth.2519.

Tanny JC, Erdjument-Bromage H, Tempst P, Allis CD. Ubiquitylation of histone H2B controls RNA polymerase II transcription elongation independently of histone H3 methylation. Genes Dev. 2007;21(7):835–847. doi:10.1101/gad.1516207.

Wang H, Dienemann C, Stützer A, Urlaub H, Cheung ACM, Cramer P. Structure of the transcription coactivator SAGA. Nature 2020;577(7792):717–720. doi:10.1038/s41586-020-1933-5.

Weake VM, Lee KK, Guelman S, Lin C-H, Seidel C, Abmayr SM, Workman JL. SAGA-mediated H2B deubiquitination controls the development of neuronal connectivity in the Drosophila visual system. EMBO J. 2008;27(2):394–405. doi:10.1038/sj.emboj.7601966.

Wyce A, Xiao T, Whelan KA, Kosman C, Walter W, Eick D, Hughes TR, Krogan NJ, Strahl BD, Berger SL. H2b ubiquitylation acts as a barrier to Ctk1 nucleosomal recruitment prior to removal by Ubp8 within a SAGA-related complex. Mol Cell. 2007;27(2):275–288. doi:10.1016/j.molcel.2007.01.035.

Xiao T, Kao CF, Krogan NJ, Sun ZW, Greenblatt JF, Osley MA, Strahl BD. Histone H2B ubiquitylation is associated with elongating RNA polymerase II. Mol Cell Biol. 2005;25(2):637–651. doi:10.1128/MCB.25.2.637-651.2005.

Yanicostas C, Barbieri E, Hibi M, Brice A, Stevanin G, Soussi-Yanicostas N. Requirement for zebrafish ataxin-7 in differentiation of photoreceptors and cerebellar neurons. PLoS One 2012;7(11):e50705. doi:10.1371/journal.pone.0050705.

Yoo SY, Pennesi ME, Weeber EJ, Xu B, Atkinson R, Chen S, Armstrong DL, Wu SM, Sweatt JD, Zoghbi HY. SCA7 knockin mice model human SCA7 and reveal gradual accumulation of mutant ataxin-7 in neurons and abnormalities in short-term plasticity. Neuron 2003;37(3):383–401. doi:10.1016/S0896-6273(02)01190-X.

Yvert G, Lindenberg KS, Devys D, Helmlinger D, Landwehrmeyer GB, Mandel JL. SCA7 mouse models show selective stabilization of mutant ataxin-7 and similar cellular responses in different neuronal cell types. Hum Mol Genet. 2001;10(16):1679–1692. doi:10.1093/hmg/10.16.1679.

Zhang XY, Varthi M, Sykes SM, Phillips C, Warzecha C, Zhu W, Wyce A, Thorne AW, Berger SL, McMahon SB. The putative cancer stem cell marker USP22 is a subunit of the human SAGA complex required for activated transcription and cell-cycle progression. Mol Cell. 2008;29(1):102–111. doi:10.1016/j.molcel.2007.12.015.

Editor: C. Kaplan